

# The Geometry of Plato's Cosmos

Mark A. Sutton

UK Centre for Ecology & Hydrology, Edinburgh Research Station,  
Bush Estate, Penicuik, Midlothian, United Kingdom, EH26 0QB. (email: [ms@ceh.ac.uk](mailto:ms@ceh.ac.uk))

## Supplementary Information

---

### S1. Supplementary Methods

#### S1.1 Construction sequence of the geometric model

Following initial recognition of its possible significance in the context of Plato's *Timaeus*, my exploration of the OED followed through five main stages:

**Stage 1** (November 2012): I constructed a first model OED, simply joining together 12 pentagonal pyramids, each being made from a hexagon of six equilateral triangles from which one triangle had been removed. This provided the basis to note the major symmetries of the OED as these related to different 'All's (5, 6, 10, 12, 30, 60, 360).

**Stage 2** (May 2013): I made a second model, this time constructing a net for each of the two hemispheres, each centred on one pentagonal pyramid, which I inscribed with equilateral triangles and Plato's scalene triangles. In reflecting on this as an image of the cosmos, with resonances to the year (i.e.,  $360^\circ$  in a circle being close to the mean of 365 days in the solar year and 354 days in the lunar year), it occurred to me to investigate how the OED could be divided into twelve months. The obvious approach was to set a point where six equilateral triangles join as the celestial North Pole, with a similar point opposite as the South Pole.

Marking out 12 sectors from each of the poles showed that there were six primary natural lines (that follow all the way between the poles), but that the intermediate (secondary) lines did not meet, requiring a diagonal step near the equator. Observation that the model offered a natural line approximating to the ecliptic ('natural geometric ecliptic', NGE, Figure 2c  $\partial-\varepsilon$ ), showed how this cut across the 12 N-S sectors, creating segments of unequal length. In addition to noting a first approximation of the galactic plane, I realised that the NGE could be divided into 36 segments of  $10^\circ$  (each of either 1 or  $\frac{1}{2}\sqrt{2}$  lengths of the shorter side of the fundamental scalene triangles, here termed a 'scalene unit', SU). These features led to the hypothesis that the OED could explain the unequal lengths along the ecliptic of the 12 zodiacal constellations.

To explore this further, I marked out the OED using the NGE ( $\partial-\varepsilon$ ) and the 1' and 2' boundaries (Figure 2c, boundaries B1, B2), aligning the model so that the most southerly point of the NGE matched to the junction of Sagittarius and Capricorn, with the most northerly point at the junction of Gemini and Cancer. A successful outcome from initial plotting of the results (see Supplementary Figure SF1) encouraged me to continue.

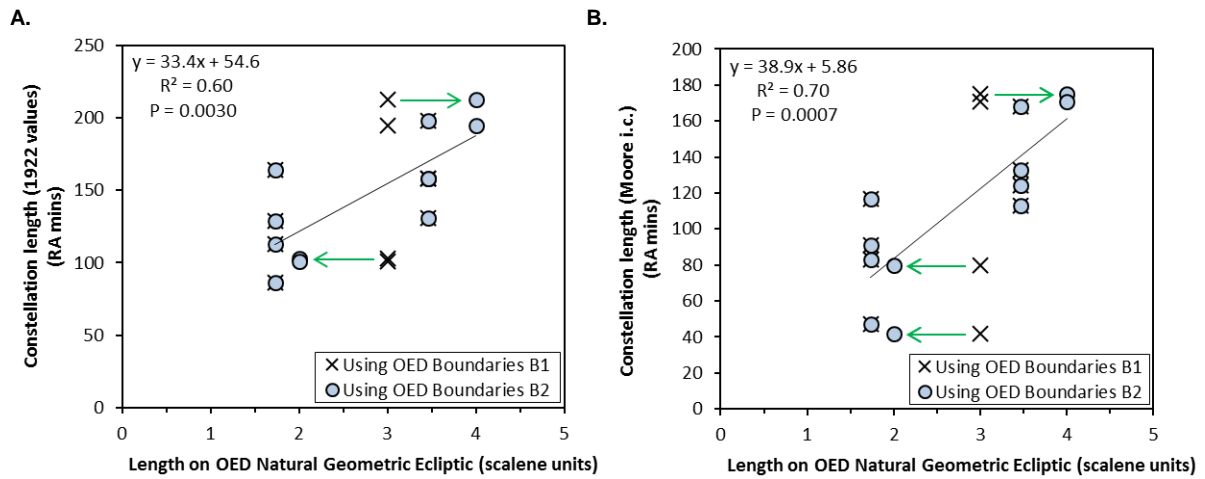
**Stage 3** (July 2013): To test the model further, I wanted to start plotting stars, for which a more robust basis of how to measure along the ecliptic (celestial longitude) and equator (right ascension), as well as north-south towards the poles, was necessary. I built a third model ( $\varnothing$  25 cm, compared with  $\varnothing$  9 cm of the previous models), marking this out with the equilateral and fundamental scalene triangles, the geometric constellation boundaries, NGE and initial galactic plane. Using this model, I explored variants for plotting the celestial equator, as far as possible following natural divisions, as a basis to consider the location of the ecliptic as compared with the NGE. Using this and the previous model, I started to explore rules for handling the junction of the 2' boundaries (Supplementary Figure SF2).

This model allowed me to start plotting stars in the vicinity of the ecliptic and equator, including the first and last stars of each zodiacal constellation. For this purpose I noted that, near the equator, the OED had a circumference 18 times the adjacent side of Plato's scalene triangle (i.e.,  $18\sqrt{3}$  SU), indicating that each degree of the equator was  $\sqrt{3}/20$  SU. Based on setting  $0^\circ$  RA in mid-Aries according to MUL.APIN, plotting the first and last stars of the zodiacal constellations (using Stellarium values) showed that the OED zodiacal sectors were consistent with a date of around 1200–1100 BCE (roughly  $\pm 400$  years). However, using a measurement system that simply followed the boundaries of Plato's scalene triangles for  $\delta$  led to substantial uncertainties further from the equator. This indicated that my initial coordinate approach was not fully satisfactory.

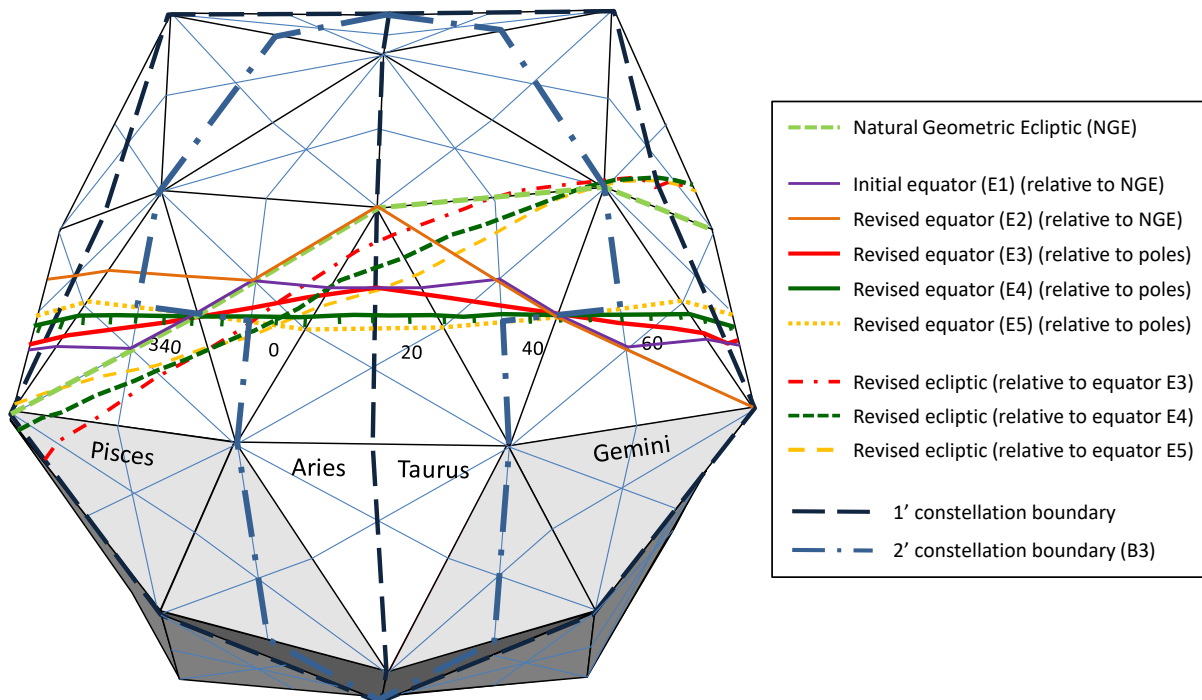
**Stage 4** (August 2013): I constructed two portable models ( $\varnothing$  5 cm and 10 cm) and used these to examine different options for marking out the celestial equator, adding in the locations of the ideal months (12 equal divisions). A key advance was made when I ceased to focus only on the NGE (which did not provide a perfect solution for mapping the ecliptic), and instead realised that the NGE could form part of the upper and lower boundary of the Path of Anu. Following two further options for the equator (E3, E4), I selected the fifth option (E5) as this best matched the timing of the Sun's path through the Paths of Anu, Enlil and Ea (see Supplementary Section 2.1 below).

**Stage 5** (August 2013): The identification of equator E5 led swiftly to the next steps. It was now possible to show how the central location of the equator within the geometric Path of Anu provided the basis for a robust measure of both RA and  $\delta$  (see next section). At the same time, this allowed me to envisage a net for the OED that centred on the Path of Anu (i.e., the primary set of 18 equilateral triangles, from which the other triangles could be mapped north and southwards). I initially struggled to make a system following the OED boundaries based on  $5^\circ$  divisions of  $\delta$ , until I noticed that steps of  $6^\circ$   $\delta$  provided a more natural division of the OED. Together with the  $5^\circ$  division of RA, this allowed a new projection to be made on which to plot the constellations, and from which I constructed a fifth model.

Subsequent investigation and analysis used printed OED models made from folded nets.



**Supplementary Figure SF1:** Comparison of sector lengths along the OED natural geometric ecliptic with constellation lengths as Right Ascension (RA). **A.** Values of RA based on modern constellation boundaries (labelled 1922 values, Moore 1974, p. 147); **B.** Values of RA based on first and last stars of constellation nets marked by Moore 1974, inside cover, i.c.). Green arrows indicate the improvement of OED estimates for the equinoctial constellations when using the 2' boundaries B2 (plotted circles) rather than B1 (plotted crosses). The summary statistics and best-fit line refer to the model values using the B2 boundaries.



**Supplementary Figure SF2:** Visualization of the OED cosmos from the outside looking in, illustrating the options explored for locating the ecliptic and the celestial equator (see Supplementary Table ST 1). Equator E1 is based on 0° RA being set at the start of the 30-day month of Aries/Nisannu, while equator E2 is based on 0° RA at the mid-point of the 20° geometric sector of Aries. Equators E3, E4 and E5 are plotted here with 0° RA as the mid-point of the 30-day month of Aries/Nisannu, for which RA values around equator E5 are shown.

## S1.2. Mapping out the Orbicular Elevated Dodecahedron

### a. Defining the boundaries of the zodiacal sectors

Having divided the OED at the N and S celestial poles into twelve sectors (Stage 2 above), the first mapping challenge was to establish how the six secondary lines should be joined

near the equator. My initial assumption was that this should be done equitably between N and S and that the natural lines of the fundamental scalene triangles should be followed as far as possible (Figure 2c,  $\beta-\gamma$ , boundary B1). According to this approach, the length of the zodiac constellation sectors along the NGE were distinguished into long ( $2\sqrt{3}$  SU), short ( $\sqrt{3}$  SU) and intermediate (3 SU). This showed some relationship with the measured constellation lengths, but there was substantial scatter introduced by the medium length constellations (Pisces, Aries, Virgo and Libra) near the equinoxes (Supplementary Figure SF1). Further consideration showed that for the other eight constellations, the division was not sensitive to the scheme used to set the N-S 2' boundaries near the equator; only for the equinoctial constellations were the results sensitive to the scheme used.

I tested several approaches, with the intention that a simple rule should be followed, settling on the following: in the first half of the year (while the sun is ascending), subtend a line from the S pole to the equator, and then follow the edge of the nearest Platonic scalene triangle to a line which then subtends to directly to the N pole (see Figure 2c,  $\beta-\gamma$ , boundary B2); in the second half of the year (while the sun is descending), the opposite approach is used to subtend first from the S pole to the equator. I subsequently noted that this simplified to: the diagonal junctions from spring to autumn equinoxes are north of the equator, while those from autumn to spring equinoxes are south of the equator, the diagonals in all cases lying within the Path of Anu. As a result of this change, Aries and Libra become short signs (2 SU), while Pisces and Virgo become the longest signs (4 SU) along the NGE.

At Stage 5, I later considered the case for an alternative rule for subtending the 2' boundaries between the N and S poles (Figure 2c, boundary B3). In plotting the celestial equator as the mid-point of the Path of Anu (equator E5), the rule to locate the 2' boundaries was as follows: subtend the 2' lines from the N pole to the equator following the edges of the Platonic scalene triangles, then move  $20^\circ$  directly east or west to the other 2' natural line, which then continues directly to the S pole.

### **b. Defining the location of the equator**

In my first efforts in Stages 2 and 3, it seemed obvious that the NGE offered by the OED would have been exploited by the ancient Mesopotamian astronomers. By contrast, the OED appeared to lack an obvious natural equator. In a first option (Supplementary Figure SF2, equator E1), I used the NGE as a basis to set the location of the equator. For equator E1, I followed the boundaries of the scalene triangles, at some points allowing a new boundary by rotating two such triangles by  $60^\circ$ . For this purpose, I allowed nine units of  $\sim 10^\circ$   $\delta$  (approximated by either 1 SU or  $\sqrt{3}/2$  SU) between the N and S poles and the equator. Although simple, this did not fit well to the actual path of the ecliptic, while also implying equinoxes at the end of Pisces and Virgo, which I considered would be too early in the year if the hypothesized Mesopotamian origin should be correct.

For a second option (Supplementary Figure SF2, equator E2), I again followed the natural lines of the scalene triangles relative to the NGE, but shifted the equinox point to be zero at mid-Aries, which provided a system more consistent with the curve of the Sun's path. I found

that the key drawback of such tuning is that it becomes impossible to map consistently all the way to the N and S poles.

As noted above, in Stage 4, I replaced use of the NGE as a reference with the idea that the line  $\beta-\varepsilon$  formed part of the upper boundary of the Path of Anu. I then considered three further options for locating the celestial equator.

For equator E3 (Supplementary Figure SF2), I assumed that the equator was midway between the poles in terms of numbers of scalene triangles, making the approximation that both 1 SU and  $\sqrt{3}/2$  SU were equivalent to  $10^\circ$  declination. (This is similar to equator E1, except that E1 was referenced to the NGE). Using this approach, I marked up the points where the 1' N-S boundaries meet the equator, as well as the midpoints of the 2' N-S boundaries using scheme B1 in order to locate the equator.

As equator E3 has the drawback of not being exact, I marked out a further equator (Supplementary Figure 2, equator E4), which was intermediate between the poles using the exact lengths of the scalene triangles. At the 1' boundary lines this gave  $\frac{1}{2}(6 + 6\sqrt{3})$  SU from pole to pole, i.e. exactly  $3 + 3\sqrt{3}$  SU between the equator and the poles. In this exact approach the equator did not easily follow the natural OED divisions.

Finally, I tested the N-S line exactly midway between the tops of the pentagonal pyramids along the E-W ring of equilateral triangles identified above as the Path of Anu, giving a fifth option (Supplementary Figure SF2, equator E5). It turned out that equator E5 was also exactly mid-way between the poles, but at other points than I had previously measured.

In evaluating these options, I considered that the 'ideal equator' used by the Mesopotamian astronomers would be: a) based as far as possible on natural divisions in the OED, and b) accurate rather than approximate. On this basis and considering the comparison with MUL.APIN, Supplementary Table ST1 summarizes the performance of the different equators that I tested. Of the options considered, equator E5 performed the best overall. It also allowed the revised net to be drawn, from which it became clear that this projection of the OED was a natural choice for mapping with an easy division to  $6^\circ \delta$ .

In retrospect (especially once seen as a flat net), the choice of equator E5 may seem obvious. I can only say that it was not obvious at first, especially given of the attraction of the NGE and the skew nature of equator E5 when visualized in three dimensions.

### **S1.3. Overall Evaluation Criteria**

One of the core challenges in the history of science is to evaluate the robustness of any conclusion. This is particularly relevant in the present study, where the conclusions are potentially contentious in relation to prevailing scholarly opinion. Two distinct aspects may be noted. First, and most important, is the need to consider whether conclusions, such as the noted geometrical correspondences, are significant/meaningful, rather than simply chance coincidences. If so, it then becomes important to be clear about the limits of what the results reveal about ancient ideas.

**Supplementary Table ST1:** Comparison of possible locations for the celestial equator on the OED model in relation to four specific criteria applied to five options E1 to E5.

Option	Based easily on the OED natural boundaries?	Accurate rather than approximate?	Agreement with MUL.APIN (II Gap A 1–7)	Natural basis for calculating declination	Other comments
Equator E1	yes	no	no	no	$10^\circ \delta$ represented by both 1 and $\frac{1}{2}\sqrt{3}$
Equator E2	yes	no	no	no	A closer fit to ecliptic than Equator. 1, but not consistent at poles.
Equator E3	yes	no	within $\pm 15$ days	no	This is an interpolated variant of Equator 1.
Equator E4	yes (but complex)	yes	within $\pm 5$ –10 days	not clear	Exact, but complicated to calculate and use.
Equator E5	yes	yes	within $\pm 5$ days	yes	Becomes the obvious choice once the appropriate net is viewed.

In order to address the first of these aspects, nine evaluation criteria were identified (*Elevated dodecahedron*, forthcoming, 2021). Eight of these criteria were already identified at the outset of that study, with the ninth being formulated at the end of that study. The criteria are as follows:

**Criterion 1: Inclusion of a coherent theoretical underpinning in relation to context.** The purpose is to demonstrate that the case to be presented flows logically from a reasoned underpinning framework. For example, the argument may contain a fresh interpretation of existing evidence, leading to the expectation necessary to frame certain hypotheses.

**Criterion 2: Inclusion of quantitative evidence that is applied to provide statistical assessment.** The strongest cases are likely to be underpinned by formal statistical testing of whether certain features could have occurred by chance. Such tests should enable acceptance of an ‘alternative hypothesis’, with a specified level of probability (e.g.,  $P < 0.05$ , with 95% confidence that the result did not occur by chance), thereby allowing a ‘null hypothesis’ (that the finding was simply chance) to be rejected. Although  $P = 0.05$  is a widely used standard, it is arbitrary and other thresholds may be adopted.

**Criterion 3: Inclusion of qualitative evidence in relation to one or more features.** Qualitative data may not be amenable to statistics, yet form the core of a case. Even with qualitative data, an indication of uncertainty should ideally be given to distinguish different strands of evidence.

**Criterion 4: Inclusion of multiple layers of evidence that together establish a coherent picture.** On their own, a few individual outcomes may occur by chance. This highlights the need to combine multiple layers of evidence to demonstrate robustness. Simple statistical concepts may be helpful. For example, if a ‘positive’ observation is assigned 50% probability of chance occurrence (e.g., testing if a tossed coin is ‘loaded’), then it requires five positive observations to give 95% confidence that the result was not by chance ( $P = 0.5^5 = 0.031$ ). With care, such approaches may be applied to qualitative data, if only to show that many coincidences are needed to make a convincing case.

**Criterion 5: Linking of a sequence of several steps of evidence, showing predictive capability.** A degree of predictive capability may be demonstrated by showing the sequence

of findings, where earlier conclusions are subsequently found to be supported or extended by later evidence.

**Criterion 6: Inclusion of a quantitative/qualitative model as a basis for robust predictive capability.** A case can be substantially strengthened where it includes a model with predictive capability based on known assumptions. For example, a mathematical or geometric model will have necessary consequences, which it may be possible to test in comparison with empirical data.

**Criterion 7: Ability to demonstrate expected degradation of the model.** This can be considered as a special case of Criterion 6. In effect, if the model is robust, then it should also be understandable how the model performance will degrade under known conditions. Put another way, the demonstration of such expected degradation provides further evidence for the soundness of the model itself.

**Criterion 8: Demonstration of an internally consistent whole.** This criterion does not guarantee robustness, but is a pre-requisite, especially if the proposed model is to be recognized as an acceptable alternative to one or more well-established positions.

**Additional Criterion 9: That the finding is not overly dependent on altering the original sources.** A proposed case to defend a certain reading should not be unduly dependent on emending primary texts or adversely criticizing the original authors. The tendency to emend/criticize to allow an easy answer may be contrasted with the opportunity to embrace difficult texts as puzzles to be solved.

As part of the parallel examination of written sources (*Elevated dodecahedron*, forthcoming), these criteria were applied to consider two questions:

- Q1) Was there historical awareness of the OED as a cosmological model?
- Q2) Was the OED recognized as a basis to map the heavens?

While written evidence from Plato to Ficino gave strong support to affirm Q1, it did not prove sufficient to affirm Q2. In the Supplementary Discussion, Q2 is re-considered using evidence from the present study. A third question is then addressed:

- Q3) Does awareness of the OED model by the ancients indicate early use of geometrical approaches?

Standard parametric statistical tests are applied here including unpaired t-tests, correlation and regression, where  $n$  refers to sample size;  $R^2$  refers to the correlation coefficient (from 0 to 1, which as a percentage is used to express the amount of variation explained);  $P$  refers to probability (from 0 to 1), with confidence estimates  $(1-P)$  expressed as percentages.

## **S2. Supplementary Results**

### **S2.1. Comparison of the OED ecliptic with MUL.APIN**

The cuneiform compendium MUL.APIN (Tablet II Gap A 1 to 7) (Hunger and Pingree 1989, pp. 88–89) gives the following account of the passage of the Sun through the paths of Anu, Enlil, Anu and Ea:

From the 1<sup>st</sup> of Addaru [month XII, i.e. start Pisces] until the 30<sup>th</sup> of Ajjaru [month II, i.e. end Taurus] the Sun stands in the path of the Anu stars; wind and weather.

From the 1<sup>st</sup> of Simanu [month III, i.e. start Gemini] until the 30<sup>th</sup> of Abu [month V, i.e. end Leo] the Sun stands in the path of the Enlil stars; harvest and heat.

From the 1<sup>st</sup> of Ululu [month VI, i.e. start Virgo] until the 30<sup>th</sup> of Arahšamnu [month VIII, i.e. end Scorpio] the Sun stands in the path of the Anu stars; wind and weather.

From the 1<sup>st</sup> of Kislimu [month IX, i.e. start Sagittarius] until the 30<sup>th</sup> of Šabatu [month XI, i.e. end Aquarius] the Sun stands in the path of the Ea stars; cold.

Based on plotting 0° RA in the middle of the 30 day zodiac sign (month) of Aries, the OED model agrees within 5 days of these dates, which would be exact where the Path of Anu is  $\pm 17^\circ$ . It was against this measure that I selected equator E5 as the closest fit (see Supplementary Table ST1).

However, if the OED model is plotted with 0° RA in the middle of the 20° geometric sector of Aries, the model fits exactly to the sense of the MUL.APIN text if each month is identified with its corresponding zodiac constellation, according to the 20° and 40° geometric sectors of each. The comments added in square brackets clarify this identification, which may be compared with the position of the actual ecliptic for 1200 BCE (Figures 4 and 5).

## **S2.2. Comparison of the OED model with modern values of constellation lengths**

### **a. Initial analysis using the OED model constellation boundary B1**

As indicated in Section S1.1, I first compared the constellation sectors of the OED model based on the NGE using boundary B1 (Supplementary Figure SF1) with the RA values of the modern constellations and boundaries as given by Moore (1974, pp. 147). The relationship was not statistically significant ( $n=12$ ,  $R^2=0.17$ ,  $P=0.19$ , crosses on Supplementary Figure SF1a).

I repeated this test using the RA lengths of the constellation published by Moore (1974, inside covers). For this purpose, I measured RA of the first and last stars according to Moore's constellation maps. I recognized that this approach had the advantage of discounting space around the major stars of each constellation, which was conversely included within the official constellation boundaries. While both ways of measurement had the disadvantage of being modern (introducing errors associated with precession), they correspondingly had an advantage in objectivity, since I felt it safe to assume that these constellation boundaries would have been published by people without knowledge of the OED model, yet would contain the possibility to have been influenced by ancient astronomers who *were* using the OED model. Again there was also no significant correlation between the OED constellation sectors along the NGE and the RA values of Moore (1974, inside covers) ( $n=12$ ,  $R^2=0.23$ ;  $P=0.12$ ) (crosses shown in Supplementary Figure SF1.b).

In considering these results, I noticed that the poor performance of the model was partly due to large scatter for the medium sized constellations (3 SU along the NGE). Realising that these were the equinoctial constellations, where choice of boundary B1 introduced uncertainty in the OED constellation sectors (Pisces, Aries, Virgo, Libra), I restricted my assessment to the remaining four short sectors (Gemini, Cancer, Sagittarius, Capricorn) and four long sectors (Taurus, Leo, Scorpio, Aquarius) of the OED model.

Using the modern constellation boundaries (Moore 1974, p. 147), the mean length of the short constellations (123 minutes RA) was found to be less than that of the long constellations (161 minutes RA) as identified according to the OED model, with this difference approaching significance at the  $P=0.05$  level ( $n=4,4$ ;  $P=0.062$ , one-tail t-test). In addition, when using the measured outlines from the constellation maps published by Moore (1974, inside covers) the mean length for the short constellations (84.5 minutes RA) was found to be significantly less than that of the long constellations (134.5 minutes RA) ( $n=4,4$ ,  $P=0.018$ , one-tail t-test). Considering these comparisons (which made no assumptions about the equinoctial constellations), I felt justified to investigate alternative OED model boundaries for the equinoctial constellations.

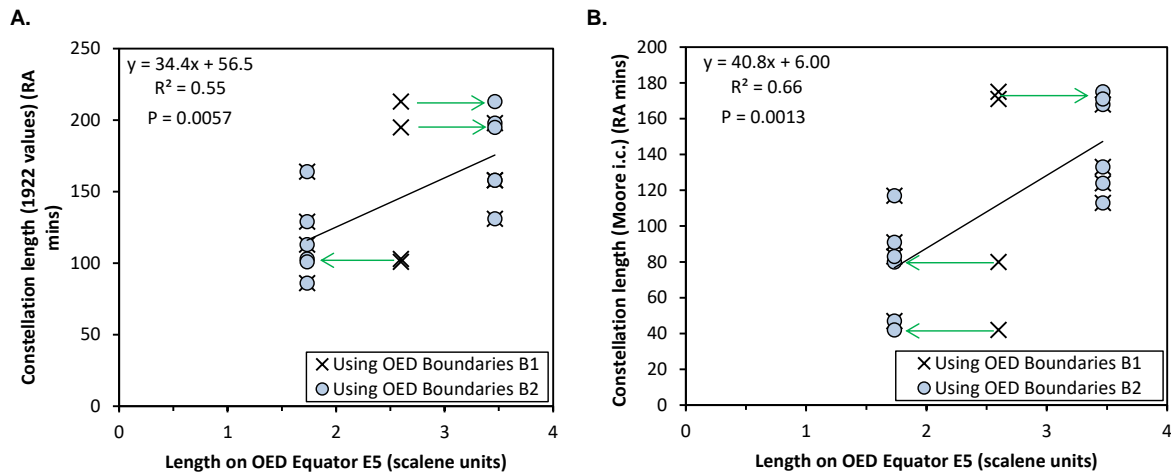
### **b. Revised analysis using the OED model constellation boundary B2**

The amendment from the OED 2' boundary B1 to B2 affects the adjacent constellation pairs Pisces and Aries, Virgo and Libra with the result that Aries and Libra become modelled on the OED as short constellations (2 SU along the NGE), while Pisces and Virgo become long constellations (4 SU). Use of boundary B2 substantially improved the performance of the geometric model, as shown in Supplementary Figure SF1 (plotted circles). Horizontal green arrows shown on these figures illustrate how the model estimates for Pisces, Aries, Virgo and Libra come closer to the modern constellation lengths. Testing for correlation using the formal constellation boundaries (Moore 1974, pp. 147) gave  $R^2=0.60$ ,  $n=12$ ,  $P=0.0030$ . Using the first and last stars measured from the printed constellation maps (Moore 1974, inside covers) gave  $R^2=0.70$ ,  $n=12$ ,  $P=0.0007$ .

### **c. Performance when matching the geometric OED model RA to measured RA**

As may be noticed, my initial estimates were based on comparing lengths along the OED NGE with modern published values of RA measured around the equator. This may lead to errors because of different orientation of the ecliptic and equator.

I therefore also compare here the OED model estimates for RA as measured in scalene units around equator E5 against the RA estimates from Moore (1974) (Supplementary Figure SF3). Again the results are statistically significant, with  $P=0.0057$  and  $P=0.0013$  for the formal constellation boundaries and the constellation maps, respectively. It is notable that this comparison as RA gave a poorer performance than the comparison along the NGE (Supplementary Figure SF1).



**Supplementary Figure SF3:** Comparison of sector lengths along equator E5 of the OED model with modern constellation lengths as Right Ascension (RA). **A.** Values of RA based on the modern constellation boundaries (1922 labelled values, Moore 1974, pp. 147); **B.** Values of RA based on first and last stars of constellations maps of Moore 1974, inside covers, i.c.). Green arrows indicate the improved OED estimates for the equinoctial constellations when using boundaries B2 (plotted circles) rather than B1 (plotted crosses) (see Figure 2c). The summary statistics and best-fit line refer to the model values using the B2 boundaries.

#### d. Effects of uncertainty in the constellation boundaries

The initial comparisons in Supplementary Figures SF1 and SF3 are dependent on the modern outlines continuing to represent the constellations originally designed by the ancient astronomers. The boundaries of many of the constellations are clearly defined, so these can be expected to have had only minor changes since ancient times. For example, although Libra was referred to by Aratus as the claws of Scorpio, it was nevertheless a distinct constellation, which was also known as the Scales (Libra) by earlier Mesopotamian astronomers (Hunger and Pingree, 1989), with its outline being restricted by neighbouring constellations.

The zodiac constellation with most uncertainty is Sagittarius, since in ancient times it was sometimes viewed as a centaur (a 4-legged man-horse) and sometimes as a satyr (a 2-legged man-goat) (*Phaenomena* 306, Aratus, 1921, pp. 405; Black and Green, 1992, pp. 65-66; van der Weerden, 1974). It therefore remains an open question what form of Sagittarius (named Pabilsag by the Mesopotamian astronomers) would have been envisaged by those who we suppose first used OED geometry to outline the zodiac constellations.

Based on the outlines of Moore (1974), Supplementary Figures SF1 and SF3 both assume that Sagittarius is a centaur, including the fainter rear stars of Sagittarius' horse body. Based on Moore (1974), Sagittarius is 164 minutes RA long when using the formal constellation boundaries and or 117 minutes according to the constellation maps (inside covers), respectively. By contrast, if we consider Sagittarius as a satyr (using the outline given by Lovi 1998, i.e. from  $\gamma$  Sgr to  $\tau$  Sgr) then Sagittarius is only 75 minutes RA.

Considering Sagittarius as a satyr improves the correlation between the OED model and the values of Moore from  $R^2=0.70$  (Supplementary Figure SF1b) to  $R^2=0.81$  ( $n=12$ ,  $P=0.0001$ ). Simply removing this point as uncertain gives a similar result, with  $R^2=0.80$  ( $n=11$ ,  $P=0.0001$ , i.e. 99.99% confidence that it is not a chance result). For clarity the individual constellation values used in Sections 2.2a to 2.2c are listed in Supplementary Table ST2.

**Supplementary Table ST2:** Summary of initial values used to assess relationships between the OED model and modern the constellation boundaries. The effect of plotting only the brightest stars of Sagittarius (i.e., as a satyr) according to the outline of Lovi (1988) is shown at the bottom.

Constellation	OED model values using 2' boundary B1		OED model values using 2' boundary B2		Right Ascension (RA) values from Moore (1974, 147): modern constellation boundaries					Right Ascension (RA) values from Moore (1974, inside covers): constellation maps				
	Scalene units on ecliptic	Scalene units on Equator E5	Scalene units on ecliptic	Scalene units on Equator E5	Start		End		difference	Start		End		Difference
					(hour)	(min)	(hour)	(min)	(min)	(hour)	(min)	(hour)	(min)	(min)
Aries (Ari)	3.00	2.60	2.00	1.73	1	44	3	27	103	1	50	3	10	80
Taurus (Tau)	3.46	3.46	3.46	3.46	3	20	5	58	158	3	25	5	38	133
Gemini (Gem)	1.73	1.73	1.73	1.73	5	57	8	6	129	6	23	7	46	83
Cancer (Cnc)	1.73	1.73	1.73	1.73	7	53	9	19	86	8	10	8	57	47
Leo (Leo)	3.46	3.46	3.46	3.46	9	18	11	56	158	9	43	11	47	124
Virgo (Vir)	3.00	2.60	4.00	3.46	11	35	15	8	213	11	52	14	47	175
Libra (Lib)	3.00	2.60	2.00	1.73	14	18	15	59	101	14	54	15	36	42
Scorpio (Sco)	3.46	3.46	3.46	3.46	15	44	17	55	131	15	57	17	50	113
Sagittarius (Sgr)	1.73	1.73	1.73	1.73	17	41	20	25	164	18	8	20	5	117
Capricorn (Cap)	1.73	1.73	1.73	1.73	20	4	21	57	113	20	22	21	53	91
Aquarius (Aqr)	3.46	3.46	3.46	3.46	20	36	23	54	198	20	52	23	40	168
Pisces (Psc)	3.00	2.60	4.00	3.46	22	49	2	4	195	23	6	1	57	171
Sgr (as satyr)										18	8	19	23	75

### e. Relationships between the geometric model and historical constellation outlines

The extent of correlation between the OED model and the estimated constellation lengths was found to be significant whether the modern values (Moore, 1974) or estimates for 1200 BCE are used. This is unsurprising given that the constellation lengths calculated by the different approaches are themselves highly correlated (Supplementary Table ST3). The lowest correlation has an  $R^2$  of 0.78 (between the two forms of the Stellarium estimates used), while the highest correlation is between the RA values of Moore (1974, inside cover constellation maps) and the Stellarium estimates of constellation length based on longitude for 1200 BCE.

**Supplementary Table ST3:** Correlation between four estimates of zodiac constellation length, expressed in either Right Ascension (RA) or longitude. Values of  $R^2$  are shown based on parametric linear regression, where  $n=12$ .

	Variable a	Variable b	Variable c	Variable d
Variable a	-	0.93	0.82	0.92
Variable b		-	0.82	0.93
Variable c			-	0.78

Variable a: RA (Moore, 1974, pp. 147), based on the modern constellation boundaries;

Variable b: RA (Moore, 1974, inside cover), based on first and last stars from the printed constellation maps;

Variable c: RA, based on first and last stars from Stellarium 0.12.1 for 1200 BCE;

Variable d: As variable c, but using longitude estimates.

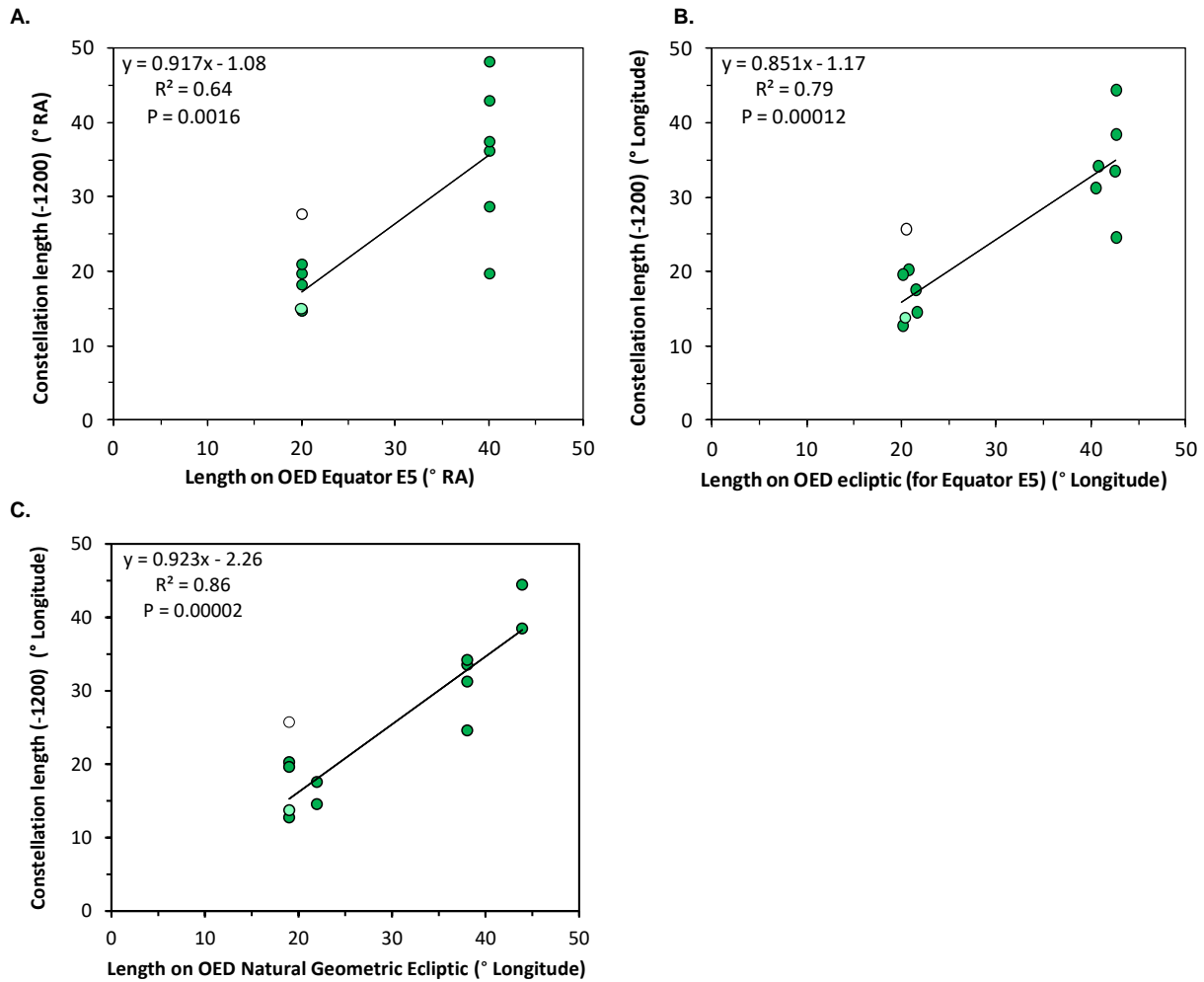
Notwithstanding the similarities highlighted in Supplementary Table ST3, it was nevertheless of interest to see how the Stellarium values for 1200 BCE compared with the OED geometric model estimates of the constellation sectors. A full listing of the constellation estimates using Stellarium as compared with different formats of the model values is given in Supplementary Table ST4. For this part of the analysis, I converted both the model and measured estimates into degrees to allow easy comparison.

The key relationships are shown in Supplementary Figure SF4. Expressed in terms of RA, the OED model constellation sectors are  $20^\circ$  or  $40^\circ$ . Comparison of these model values with the Stellarium estimated RA values for 1200 BCE showed that they were significantly correlated ( $R^2=0.64$ ,  $n=12$ ,  $P=0.016$ ), with most uncertainty associated with those constellations categorized as long sectors in the OED model (Supplementary Figure SF4a).

Using the OED sectors along the actual ecliptic (based on equator E5 with model boundaries B3) gave an improved relationship with the Stellarium longitude estimates ( $R^2=0.79$ ,  $n=12$ ,  $P=0.00012$ ; Supplementary Figure SF4b). The best relationship, however, was found when comparing the Stellarium longitude estimates with the constellation sectors based on the NGE of the OED model (using boundaries B2). In this case, 86% of the variation in constellation length was explained by the OED model sectors if Sagittarius is taken as a satyr ( $R^2=0.86$ ,  $n=12$ ;  $P=0.000014$ ) and 77% of the variation if Sagittarius is taken as a centaur ( $R^2=0.77$ ,  $n=12$ ;  $P=0.00019$ ), see Supplementary Figure SF4c. While recognizing the uncertainty in Sagittarius, if the 2' boundaries B2 are accepted as justified, then there is 99.981–99.999% confidence that this relationship around the NGE is not the result of chance. (If Sagittarius were excluded, this would give  $R^2=0.84$ ,  $n=11$ ,  $P=0.000066$ , i.e. 99.993% confidence.)

**Supplementary Table ST4:** Summary estimated constellation lengths according to the geometric OED model and as calculated using Stellarium 0.12.1 for 1200 BCE at a location 36 °N for both Right Ascension (RA) and celestial longitude. Stellarium estimates of declination ( $\delta$ ) are also shown. (Degrees are shown in decimal format.)

Constellation	First and last star (by RA)	OED model values			Right Ascension (RA)			Decl.	Longitude	
		Range of RA on equator E5 (°)	Range of longitude on natural geometric ecliptic (°)	Range of longitude on ecliptic using Equator E5 (°)	RA time (time, h:m)	RA (°)	Last - first (°)	$\delta$ (°)	Longitude (°)	Last - First, (°)
Aries	$\gamma$ Ari (Mesarthim)				23:06	346.5		2.1	33.1	
	$\delta$ Ari (Botein)	20	22.0	21.4	00:19	4.8	18.3	4.1	50.7	17.6
Taurus	$\omicron$ Tau				00:39	9.8		-5.9	51.2	
	$\zeta$ Tau	40	38.0	42.4	02:34	38.5	28.8	12.8	84.7	33.5
Gemini	$\nu$ Gem (Propus)				03:36	46.5		16.6	93.4	
	$\beta$ Gem (Pollux)	20	19.0	20.6	04:25	66.3	19.8	28.7	113.7	20.3
Cancer	$\chi$ Cnc				04:56	74.0		30.5	120.8	
	$\alpha$ Cnc (Acubens)	20	19.0	20.0	05:55	88.8	14.8	18.4	133.5	12.8
Leo	$\epsilon$ Leo				06:29	97.3		33.0	140.7	
	$\beta$ Leo (Denebola)	40	38.0	40.4	08:54	133.5	36.3	30.5	172.0	31.3
Virgo	$\nu$ Vir				08:53	133.3		22.5	174.1	
	109 Vir	40	43.9	42.6	11:06	181.5	48.3	18.1	218.5	44.4
Libra	$\alpha$ Lib (Zubenelgenubi)				12:02	180.5		-0.2	225.2	
	$\theta$ Lib	20	22.0	21.5	13:02	195.3	14.8	-2.9	239.8	14.6
Scorpius	$\pi$ Sco				12:59	194.8		-11.8	243.0	
	$\iota$ Sco	40	38.0	42.6	14:18	214.5	19.8	-31.5	267.6	24.6
Sagittarius	$\gamma$ Sgr (Alnasl)				14:48	222.0		-23.3	271.3	
	$\tau$ Sgr (back of satyr)	20	19.0	20.4	15:48	237.0	15.0	-25.0	285.0	13.7
	$\varsigma$ Sgr (hind of centaur)	20	19.0	20.4	16:39	249.8	27.8	-29.3	297.0	25.7
Capricorn	$\alpha$ Cap				17:15	258.8		-16.1	303.8	
	$\delta$ Cap (Deneb Algedi)	20	19.0	20.0	18:39	279.8	21.0	-25.4	323.4	19.6
Aquarius	$\epsilon$ Aqr (Albali)				17:48	267.0		-15.3	311.7	
	$\psi$ Aqr	40	38.0	40.7	20:18	304.5	37.5	-23.6	345.9	34.2
Pisces	$\gamma$ Psc				20:26	306.5		-11.5	350.8	
	$\alpha$ Psc (Alrescha)	40	43.9	42.6	23:18	349.5	43.0	-14.4	29.3	38.5



**Supplementary Figure SF4:** Comparison of lengths of the zodiacal constellation sectors from the OED geometric model with actual constellation lengths estimated using Stellarium software (for 1200 BCE). **A.** Model values based on Right Ascension (RA, measured along the equator) using OED equator E5 compared with Stellarium RA values; **B.** Model values based on longitude (measured along the ecliptic) from the OED ecliptic referenced to equator E5 compared with Stellarium longitude values; **C.** Model values based on the NGE of the OED (using 2' boundaries B2) compared with Stellarium longitude values. The regression lines are here calculated using Sagittarius as a 2-legged satyr (light green circles, outline from Lovi, 1988), while the value for Sagittarius as a 4-legged centaur is also shown (white circles).

By excluding the zodiac constellations near the equinoxes the performance of the OED model can be assessed without any assumptions (i.e., whether to use the 2' Boundaries B1 or B2). Supplementary Table ST5 shows that in the absence of any assumptions, the OED correctly predicts Taurus, Leo, Scorpius and Aquarius as 'long constellations' and Gemini, Cancer, Sagittarius and Capricorn as 'short constellations'. The results are statistically significant ( $P < 0.05$ ) whether the constellations are measured using Right Ascension or celestial longitude, or whether Sagittarius is measured as a satyr or centaur. Again the best performance is for longitude with 99.2–99.9% confidence that it is not a chance result.

**Supplementary Table ST5:** Comparison of constellations predicted by the OED model to be long versus those predicted to be short, excluding the constellations near the equinoxes (Ari, Vir, Lib, Psc), thereby excluding any assumptions related to use of 2<sup>+</sup> Boundaries B1 or B2/B3. The constellation values are taken from Supplementary Table ST4. Values assume Sagittarius as a satyr, or in [ ] as a centaur.

Constellation	OED model prediction	Length as Right-Ascension (last-first star, °)	Length as Longitude (last-first star, °)
Taurus	Long	28.8	33.5
Leo	Long	36.3	31.3
Scorpius	Long	19.8	24.6
Aquarius	Long	37.5	34.2
Gemini	Short	19.8	20.3
Cancer	Short	14.8	12.8
Sagittarius as satyr [as centaur]	Short	15.0 [26.8]	13.7 [25.7]
Capricorn	Short	21.0	19.6
Means	Long	30.6 [30.6]	30.9 [30.9]
	Short	17.7 [20.9]	16.6 [19.6]
Variance	Long	66.7 [66.7]	19.2 [19.2]
	Short	10.3 [28.7]	15.2 [28.0]
F-test if variances different *		P= 0.08 [0.25] (not significant)	P= 0.42 [0.38] (not significant)
Significance of one-tailed t-test that Long>Short*		P=0.013 [P=0.046]	P=0.0014 [P=0.0083]
Confidence that Long>Short constellations*		98.7% [95.4%]	99.86% [99.17%]

\* As the F-tests show that variances are not significantly different (P>0.05), the t-tests are calculated assuming equal variances.

### S3. Supplementary Discussion

#### S3.1. Background

This study developed from a reflection on Plato’s elemental polyhedra described in the *Timaeus* (especially 53c–57d; Plato 2008, pp. 46–52), informed by reading of later Platonists, such as Plutarch (1936), Olympiodorus and Damascius (1978) and Proclus (1820), refining initial ideas emerging from other work (Sutton et al. 2008, pp. 593–597; 2011, pp. 88-92). For example, Damascius refers to the dodecahedron as representing a transitional form between the other polyhedra and the sphere (*Commentary on Plato’s Phaedo*, Damascius, 1978, p. 368).

The key underlying principle was to recognize the inter-changeability of Plato’s fundamental scalene triangles (sides 1:√3:2 SU) between the elements Water, Air and Fire, with these elements being made up of 120, 48 and 24 scalene triangles, respectively. Plato points out how the elements may battle with one another so that the primary triangles re-combine to produce new forms. For example, a large amount of material with the nature of Air, Water or even Earth may triumph over a small amount of Fire, so that two tetrahedra of Fire decompose to produce one octahedron of Air. Similarly, something with the nature of Air may be dominated and broken up so that two and a half octahedra of Air recombine to form one icosahedron of Water (*Timaeus* 56e, see below). Considering that the All mentioned by

Plato (*Timaeus* 55c) might be based on the summits of the other elements (e.g., *On Plato's Timaeus* 2.56, Proclus 1820, Vol. 1, p. 469), it was logical to suppose that this form could be made by marrying scalene triangles from the other elements. Only later did I recognize that this might also be inferred from *Timaeus* 32c: 'Now of the four elements the construction of the Cosmos had taken up the whole of every one' (*Tōn de dē tettarōn hen holon hekaston eilēphen hē tou kosmou xustasis*; Plato, 1929, trans. Bury, pp. 60–61).

My own exploration of this topic originally started from a reflection on how the elements Water, Earth, Fire and Air were considered in Greek and Arabic alchemy, which show several parallels with the *Timaeus*. In alchemical context, the four elements are combined in pairs (Water plus Fire; Earth plus Air; with the products of these then combined) constituting three 'marriages'. A famous description is repeated several times throughout the *Phusika kai mustika* where: 'Nature delights in nature, nature conquers nature, nature masters nature' (*he phusis tē phusei terpetai, kai he phusis tēn phusin nika, kai he phusis tēn phusin kratei* (trans. Martelli, 2013, pp. S84–S 85). This work is traditionally attributed to Democritus, but is generally considered pseudonymous according to modern scholarship (Hershbell, 1987; Martelli, 2013, pp. S5–S7; Viano, 2018, p. 471). The three terms delight (*terpetai*), conquer (*nika*) and dominate/rule (*kratei*) appear to be associated with the three marriages, as later adopted in Arabic alchemy, such as that of al-Rāzī and al-Jildakī (see Stapleton and Azo, 1910, pp. 68–73; Sutton et al., 2020, Supplementary Material pp. 8–9). As Viano (2005, p. 99) has noted, Plato also uses words related to two of these terms (*nikan, kratein*) where he describes the mixing of the geometric elements through the primary scalene triangles (*Timaeus* 56e):

And again, when a small quantity of fire is enclosed by a large quantity of air and water, or of earth, and moves within them as they rush along, and is defeated (*nikēthen*) in its struggle and broken up, then two corpuscles of fire unite to make one form of air. And when air is defeated (*kratēthentos*) and disintegrated, from two whole forms of air and a half, one whole form of water will be compounded (Plato, *Timaeus* 56e, trans. Bury, 1929, pp. 138–139).

The limitations of Bury's translation are obvious, as both words are translated by 'defeated'. In fact, most scholars would place the earliest Greek alchemy later than Plato, with the oldest texts such as the *Phusika kai mustika* generally thought to be after 50 BCE (e.g., Martelli, 2013, p. 29; Viano, 2018, p. 471). Nevertheless, other evidence (beyond the scope of the present study), suggested to me that the origins of Greek alchemy could be much earlier than currently accepted. While acknowledging uncertainty, I recognized that the parallels between the alchemical elements and Plato's geometric elements should be further explored. In particular, since practical alchemical marriage of (the materials they referred to as) Water, Fire etc was focused on preparing alchemical aether as the quintessence, then we should expect that Plato's analogous remixing of the geometric elements (*Timaeus* 56e) would also be able to produce the geometric aether/quintessence (i.e., the dodecahedron). Encouraged by the setting of the elevated dodecahedra in the Byzantine-influenced, renaissance context of St Mark's, Venice, I gave further thought to this form and realised that the puzzle could be solved by use of the OED divided into 360 primary scalene triangles (e.g., five units of fire plus two of water would give 360 scalene triangles; the same would be achieved by one unit

of water, three of air and four of fire, etc.). As explained in Supplementary Section S1.1, this led to my geometric and astronomical investigation of the OED. Only later, was it possible to piece together a more comprehensive picture.

While some may contest the alchemical-geometric inferences above, it should be noted that these only served to inform the initial hypotheses of this study. Other points may be a matter of ongoing debate. For example, it is commonly asserted that it was Aristotle who introduced the idea of aether as the fifth element or quintessence, which makes up the immortal substance of heaven. However, this was certainly not the view of Proclus, who commented:

Aristotle discusses [things] in the first place such as pertain to the heavens, in a way conformably to Plato; so far as he calls the heaven unbegotten, and a fifth essence. For what difference is there between calling it a fifth element, or a fifth world, and a fifth figure, as Plato denominates it? (*On Plato's Timaeus* 1.1.6, Plato 1820, Vol. 1, 16, referring to *De Caelo* 270b22 of Aristotle).

Support for his interpretation can also be found in the *Phaedo*, where Plato writes about the true earth as being ‘as pure as the starry heaven in which it lies, and which is called Ether by most of our authorities. The water, mist and air are the dregs of this Ether’ (*Phaedo* 109b, Plato 1958, 146; cf. *Epinomis* 981c). The association of aether with Plato’s All appears to be because the heavens dominate the overall size of the cosmos (cf. Aristotle, *De Caelo* 278b).

The reason that Plato’s All has traditionally been identified with the simple dodecahedron is the geometric restriction to only five regular convex polyhedra, a limitation proved by Kepler (*Harmonices Mundi Libri V*, Book II.xxv, Kepler 1997, pp. 122–123). As Kepler showed, an extended network of equilateral triangles will not make a regular convex polyhedron beyond the icosahedron. The tetrahedron, octahedron and icosahedron are based on vertices joining three, four and five equilateral triangles, respectively. Combining the corners of six equilateral triangles produces a flat plane, so that five equilateral triangles is the maximum that can be joined at a vertex to form a convex polyhedron. However, this rule does not hold if the requirement to form only *convex* polyhedra is relaxed. In the OED, the compensation of concave and convex vertices allows this regular polyhedron to be formed based on equilateral triangles, and hence ultimately on Plato’s fundamental scalene triangles.

Kepler is recognized as having provided the first scientific description of the variant dodecahedron that he termed *echinus*, today known as the small stellated dodecahedron (SSD), where the component triangles combine to form 12 plane pentangle surfaces. He applied the same principle for his description of the ‘great stellated dodecahedron’ (GSD), formed by stellating the triangular faces of the simple icosahedron. Kepler realised that these shapes were ‘perfectly regular’, like the standard Platonic Solids, while containing concave adjacent surfaces (*Harmonices Mundi Libri V*, Book II.xxvi, Kepler 1997, p. 133). He also suggested that the geometry of the SSD offered an explanation of the spacing between the orbits of Mars and Venus (*Harmonices Mundi Libri V*, 5.4, Kepler 1997, p. 407). However, Kepler appears to have considered these forms to be only variants of the dodecahedron, rather than new polyhedra in their own right.

Given Kepler's attention to the SSD and GSD, while passing over the OED, it appears that he placed a higher priority on forming external plane surfaces as a condition of regularity (thereby accepting the use of stretched isosceles triangles), than for regularity based on using equilateral triangles. However, there is no *a priori* reason to maintain such a precedence, and one might equally argue that the use of equilateral triangles makes the OED more regular than the SSD. Kepler's lack of interest in the OED may simply be because it contributed no obvious proportions for his cosmic system.

The well-known *opus sectile* elevated dodecahedron in the floor of St Mark's, Venice ( $\varnothing$  37 cm) is in the north entry from the atrium to the nave (Arch of St. Peter). A second lesser-known elevated dodecahedron ( $\varnothing$  17 cm) is placed 42 m east in the central opening of the presbytery, at the high point of the basilica. Michelangelo is also credited with designing an elevated dodecahedron also placed in cosmological context (c. 1525): the golden orb surmounting the New Sacristy of the Basilica of San Lorenzo in Florence has flattened pyramids being close in form to a pentakis dodecahedron (Florence Daily News, 2013). Other elevated dodecahedra in Venice appear to be of later date (c. 1680, two SSDs with accompanying GSDs), which are set into the floor of the church of San Pantaleon.

### **S3.2. Comparison of the model with historical constellation boundaries**

Overall, the correlation between the OED sectors and the measured constellations is rather robust and little dependent on the exact form of the values used. This is to be expected given such a strong underlying relationship and the high degree of correlation between the different estimates of actual constellation length (Supplementary Table ST3). It is nevertheless interesting that there is such a clear difference in the performance of the comparison of model *versus* measurement depending on whether equatorial or ecliptic estimates are used. The closer relationship between the OED model and estimated constellation lengths in longitude compared with RA (Supplementary Figure SF4) suggests that those who set the zodiacal constellation boundaries did so primarily based on distribution along the ecliptic rather than along the equator.

Secondly, it is also interesting to see that a higher correlation is found when using the NGE (Supplementary Figure SF4c, boundaries B2) than when using the actual ecliptic (boundaries B3). This is in part due to Pisces and Virgo being the longest constellations, a feature also shown in the OED model. Other configurations of the NGE may also have been used. For example, it is possible to envisage a 'Natural Ecliptic Path'  $\pm 12^\circ$  RA wide (passing between the diagonals of boundaries B2), which would warrant further testing.

When using either the secondary boundaries B2 or B3, the geometric 'cosmic arrows' are of balanced shape for both the winter and summer positions (i.e., zones of Sagittarius and Capricorn; zones of Gemini and Cancer). By contrast, the cosmic arrows are skew for Aquarius+Pisces and Leo+Virgo when using boundaries B2 (see Figures 4 and 5). This could have re-enforced the idea of the cosmic arrows near the solstices and the Milky Way as being the primary arrows.

Other variants for the equatorial junctions of the 2' boundaries can also be envisaged. However, it should be emphasized that such uncertainties are not critical to the overall conclusions. The Mesopotamians and Greeks presumably worked through several stages just as I did. The initial boundaries of the OED that were first used to outline the constellations may therefore have been refined by later generations.

Perhaps the greatest example of such a refinement was the transformation from OED model to the spherical model of the cosmos. The date of this transformation is not well known. Such spherical geometry has often been attributed to Greek astronomers who inherited the earlier Mesopotamian traditions (c. 500–200 BCE; Brack-Bernsen 2003; Steele 2007; 2008, see also Supplementary Section S3.5). A spherical view of the cosmos is also clearly indicated by Plato (*Timaeus* 33c), forming a curious juxtaposition with his hint about the dodecahedron. Overall, the OED model as explored here points to a tradition of reserved knowledge which challenges our understanding of how and when such discoveries were made. For example, it is possible that the cultural conditions in Greece (and especially in Magna Graecia) allowed a more-open publication than in Mesopotamia. It is therefore relevant to explore hints by other ancient authors who may have known more than they were openly saying. In this way, the riddling comments of Heraclitus, Empedocles and Plato may all be seen in the context of an increase in openness, with the consequent risks of censure just as Timaeus of Tauromenium and Neanthes recorded (Diogenes Laertius, *Lives of the Philosophers* 8, 54–55).

### S3.3. Potential tuning the OED model in relation to skewness of fit

While a close correlation between the OED geometric model and constellation lengths is found, there is also a seasonal skewness, with the winter constellations set later relative to the summer constellations. Options to explain this could include:

- a. **Effect of varying atmospheric visibility.** The Mesopotamian astronomers relied to a significant extent on observations of Visible Morning Rising (VMR, or Heliacal Rising), which is the annual date of the first observation of a star from watching just before dawn. In principle VMR provides an estimate related to True Morning Rising (TMR), the date when the star and the sun rise together), but, as TMR cannot be observed, VMR is of more practical use (e.g., *Introduction to the Phenomena* XIII.6–10, Geminus 2006, p. 201). As VMR is dependent on varying atmospheric visibility, this could have led to stars being allocated to later dates in winter, as a result of poorer visibility. However, it seems unlikely that this would cover such large fraction of the year, while centuries of observations might be expected to have taken account of such variations.
- b. **Location of observation.** The relative position of stars depends on the observation point, so this might lead to some differences. Preliminary testing using Stellarium (e.g., 32° N in Babylon compared with 36° N in Assyria or Rhodes) showed differences that are too small to explain those seen observed.
- c. **Date of observation.** Due to precession, the date of observation also affects the relative positions of stars. My initial comparison of 500 and 1200 BCE indicated that this was insufficient to explain the observed differences in the OED model fit to the observations.

- d. **Seasonal variation in the path of the Sun:** The ellipticity of the Earth's orbit around the Sun means that the Sun proceeds along the ecliptic more slowly in autumn and more rapidly in spring (*Introduction to the Phenomena* I.13–17, Geminus, 2006, p. 117). Starting from the summer solstice as a reference, this effect amounts to a gain of +1.2, -3.2, -1.2, +3.2 days through each following quarter of the year. A cumulative correction for this effect in the Stellarium estimates of RA would therefore add -1.2, +2.0, +3.2, 0 days to those used in mapping for the start of Libra, Capricorn, Aries and Cancer, respectively, assuming that the Ancients mapped their constellations based on observations of VMR.

As a starting-point to investigate these points, I was interested in the estimates of van der Waerden (1974, pp. 76–77) concerning the timing of star risings based on MUL.APIN (Tablet I, ii.36–iii.12, see Hunger and Pingree, 1989, pp. 40–47), which van der Waerden dated to around 1000 BCE, at the latitude of Babylon (32° N). He compared the estimated timings with calculated estimates and found differences of several days. These differences appeared to be seasonally varying, so that several constellations were recorded in MUL.APIN as rising later than expected in winter than estimated by his calculations for 1000 BCE. This finding offered a potential connection with the seasonal skewness of the OED model.

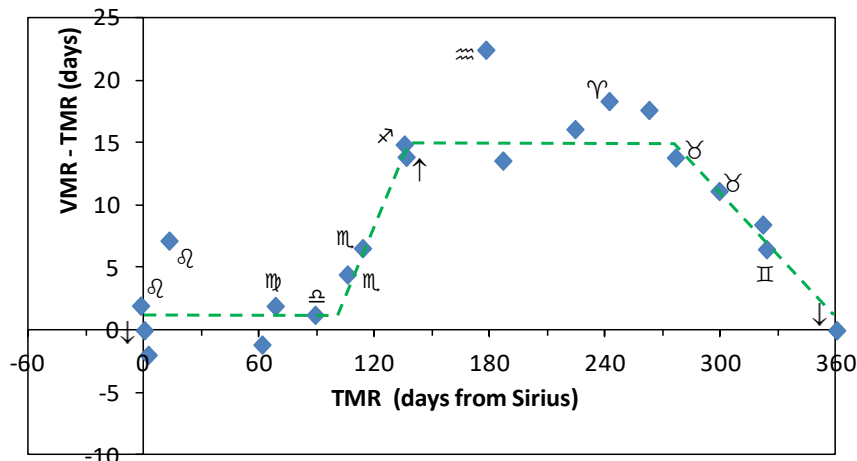
Hunger and Pingree (1989, pp. 11, 138) criticized van der Waerden's assessment, suggesting that the underpinning data from MUL.APIN were of limited use for such an analysis given the uncertainties in the constellation outlines. While we may agree for individual constellations, it was notable that Hunger and Pingree (1989) did not comment on the apparent *collective* seasonal skewness in the MUL.APIN data, and I therefore considered this dataset worth revisiting. In order to limit uncertainties, I reduced the list of stars/constellations, excluding those where the Mesopotamian boundary was most unsure. In this way I reduced van der Waerden's list of 34 constellations to 20. For consistency with the estimates of van der Waerden, I applied Stellarium software to find the date of TMR for 1000 BCE at a location 32° N, with all results normalized to Sirius as the first star of the year (van der Waerden, 1974). The results are shown in Supplementary Table ST6 and Supplementary Figure SF5.

Although different in detail from the estimates of van der Waerden (1974, pp. 76–77), the present comparison supports his contention that the MUL.APIN observations based on VMR are not evenly spaced through the year when compared with the calculated values of TMR. In particular, Supplementary Figure SF5 shows a rapidly lengthening delay following Libra (around 90 days after Sirius), so that, by the rising date of Sagittarius, there is a delay of around 15 days. This delay then lessens from the Pleiades (around 270 days after Sirius) until the delay is removed at the next rising of Sirius. The pattern of varying delay broadly matches to the position of the Milky Way (i.e., in generation and then ascent from Sirius to Aquila; in celestial separation and then descent to the body from Aquila to Sirius). However, why this should connect to a temporal shift compared with TMR remains unclear.

**Table ST6:** Comparison of dates for visible morning rising (VMR) of major stars from MUL.APIN (Tablet I, ii.36–iii.12) with estimated values of True Morning Rising (TMR) from Stellarium 0.12.1. VMR, TMR and RA are normalized to Sirius.

Babylonian name (van der Waerden (1974))	Mul Apin	Constellation	Mains star	RA calculated (Stellarium) (°)	VMR MUL.APIN (days)	TMR Calculated (Stellarium) (days)	Difference (days)
KAK.SI.DI	Arrow	Canis Major	Sirius	0	0	0	0
MUSH	Snake	Hydra	δ Hya	21	0	2	-2
UR.GU.LA	Lion	Leo	ε Leo	33	0	-2	2
LUGAL	King	Regulus	Regulus	42	20	13	7
SHU.PA		Bootes	Arcturus	111	60	61	-1
AB.SIN	Furrow	Virgo	Spica	95	70	68	2
Zibanitu	Scales	Libra	α Lib	115	90	89	1
GIR.TAB	Scorpion	Scorpio	δ Sco	130	110	106	4
GAB.GIR.TAB	Heart of Scorpion	Antares	Antares	136	120	113	7
A mushen	Eagle	Aquila	ζ Aquila	184	150	136	14
PA.BIL.SAG		Sagittarius	γ Sgr	157	150	135	15
GU.LA	Great One	Aquarius	β Aqr	214	200	178	22
IKU	Field	square of Pegasus	β Pega	243	200	186	14
KUA	Fish	Piscis Austrinis	Formalhut	230	240	224	16
LU.HUN.GA	Hired Labourer	Aries	β Aries	281	260	242	18
GAM	Crook	Auriga	Capella	321	280	262	18
MUL.MUL	Stars	Pleiades	Pleiades	307	290	276	14
is li-e	Jaw of Bull	part Taurus	Aldebaran	320	310	299	11
SIB.ZI.AN.NA	True Sheppard of Heaven	Orion	γ Orionis	334	330	324	6
MASH.TAB.BA .GAL.GAL	Great Twins	part Gemini	Castor	357	330	322	8
KAK.SI.DI	Arrow	Canis Major	Sirius	360	360	360	0

This list is restricted compared with the equivalent list of van der Waerden (1974, p. 76) to remove those constellations for which the position is most uncertain. The calculated values from Stellarium are here based on 1000 BCE in Babylon (32° N) to allow comparison with van der Waerden (1974).



**Supplementary Figure SF5:** Comparison of Visible Morning Rising (VMR) estimates from MUL.APIN (Tablet I, ii.36–iii.12, Hunger and Pingree 1989, pp. 40–47) with calculated values of True Morning Rising (TMR) using Stellarium. Values normalized to Sirius and applied for Babylon, 32°N, 1000 BCE for consistency with van der Waerden (1974, 76). The dashed line illustrates a possible step-function, while the symbols indicate the zodiac constellations (labelled according to Figure 3), Sirius (↓) and Aquila (↑) (cf. Supplementary Table ST6).

This pattern is also similar to the delay for the zodiacal constellations mapped onto the OED, though a delay increasing to around 5–10 days relative to Sirius would be a better fit than 15 days. Correcting for such an effect would tend to stretch Scorpio (which is the shortest ‘long’ constellation on the OED model), as with the smaller correction provided by option d. above. However, as with the delay the MUL.APIN data, the cause of the seasonally varying delay in the fit of the OED model remains uncertain.

It is worth to note that correcting for a delay of 5–10 days would improve the OED model fit for most of the winter and spring constellations, such as Sagittarius, Aquarius, Pisces and Aries. However, while correcting these constellations, it would increase the discrepancy for Capricorn, moving it out of its present alignment. This could be explained by:

- i. the possibility that Capricorn, as a faint constellation (not in the MUL.APIN list of VMR), has had its constellation boundary changed;
- ii. the need to refine further the geometric model (e.g., when considering the implications of plotting a Natural Ecliptic Path of  $\pm 12^\circ \delta$ );
- iii. the possibility that the composite sign Capricorn originally represented a terrestrial part (the goat) and an aquatic part (the fish), with the latter associated with Aquarius.

It is tempting to apply option d. or Supplementary Figure SF5 to make corrections to the OED model fit. However, I would consider this premature until the seasonal delays seen in MUL.APIN and in relation to the OED model are better understood.

### **S3.4. Dating of the OED model**

Given that this whole discussion of the OED points to an unpublished tradition of reserved knowledge, we should be extremely cautious about any firm dating. While several criteria may be considered, it is sufficient to note here that the effect of precession would mean that the observed pattern of long and short constellations only applies for a specific window of time. Prior to 4000 BCE the spring equinox would have occurred in the constellation of Gemini, which according to the orientation of the OED would suggest that Gemini would have been a long constellation, while Taurus would have been a short one. In the same way, the geometry of the OED would suggest that that, prior to this date, Sagittarius and Scorpio would have been long and short constellations, respectively. The implication is that the constellation fit to the OED characterized by Figure 3 was designed after 4000 BCE.

While I found that the constellations fitted well to the OED framework for 1200 BCE (Figure 4B), I have since also plotted the constellations for 1100 BCE using the same  $0^\circ$  RA reference (not shown). In this case, the fit is equally good, with slightly altered alignments worth further examination (e.g. Delphinus, Delta and the head of Sirius). It should be noted that choice of these dates 1200–1100 BCE (c.  $\pm 400$  years) is simply based on overall visual fit of the constellations to the OED. Further sensitivity testing in relation to alternative  $0^\circ$  RA reference points, as well as exploration of formal date optimization and uncertainty procedures, should be considered for future study. It would also be worth exploring the implications of the OED model further in relation to other periods and for other geometric orientations. For example, after 50 BCE the spring equinox occurred in Pisces rather than

Aries. In this context the OED model might have been amended so that Aries became a long constellation and Pisces a short constellation, with Libra and Virgo becoming long and short constellations, respectively. Partial support for such a change might be seen in the Dendera zodiacs (e.g., van der Waerden 1974, pp. 30–31), which date from the Roman period. Aries and Libra are visualized as long constellations, while Virgo is shown standing, as a short constellation. However, this would not explain the appearance at Dendera of Pisces as a long constellation. Although this application of the OED model to Dendera is therefore not sufficiently convincing, it illustrates how geometric interpretation of such images might be further explored.

### S3.5. Uncertainties concerning geometrical and arithmetical approaches

One of the challenges for the present study is the view shared by several recent scholars that doubts the extent to which Pythagorean cosmology was geometrical rather than arithmetical in approach (Netz, 2014, p. 181; Gregory, 2015, pp. 29, 42; Huffman, 2018, section 5). Such a view risks circularity in doubting Philolaus Fragment 12 (see Introduction) or in downplaying late accounts, such as Iamblichus' record of how the Pythagorean Hippasus broke silence in publishing how to make the sphere of twelve pentagons (see *The Pythagorean Life* 18, Taylor, 1818, p 232; Burkert, 1972, pp. 457–465). However, as noted in the main text, modern astronomical scholarship points to a similar picture, with Babylonian astronomy apparently restricted to arithmetical approaches and geometrical astronomy only appearing in later Greek accounts (e.g., Brack-Bernsen, 2003; Steele, 2008, p 56; Zhmud, 2012, pp. 317–322; Rochberg, 2020, pp. 313–314, 317–318). As Rochberg summarizes of Babylonian astronomy:

No geometrical dimension was attributed to the heavens in mathematical astronomical texts, whose predictive schemes were strictly arithmetical and linear, and consequently shed no light on the question of the spatial structure of the heavens (p 314)... Finally, despite the apparent lack of a conception of the celestial sphere in Babylonian astronomy, the periodic return of the planets to their synodic appearances with respect to certain points of longitude seems to presuppose the 360° circle of the ecliptic, the path of the sun. Whether it was conceived of as such, or as a repeating linear sequence of 360 points, however, is difficult to show (p. 318).

While recognizing such difficulties, it is worth noting that there is a broad spectrum from use of arithmetical approaches in a spatial context, to simple spatial/geometric constructs, to the application of classical proofs in geometry. The boundaries in such classifications are not necessarily exact and may have differed according to past and present definitions. The debate resulting from of a lack of consensus around the term 'geometric algebra' illustrates the difficulty (Høyrup, 2016, e.g. pp. 27, 34). It is also possible that scholarly interpretation of Greek vs Babylonian astronomy may have been coloured by bias between available sources, with Greek accounts including a more theoretical perspective, while the Babylonian evidence is dominated by working texts of astronomical practice. As Jones (1999, p 149) has noted: 'Babylonian predictive astronomy shows no symptoms of underlying explanatory theories, whether physical or geometrical.' It may simply have been less acceptable to write about such things in the earlier Babylonian context (cf. Schaefer, 2004, pp. 194–195; Lenzi, 2013).

Considering this perspective, it is notable that I was able to construct the three-dimensional OED model using very little geometry. Starting with the basic geometric construction of an equilateral triangle (Euclid, *Elements* 1.1, with no need for the proof), I created a net of 60 equilateral triangles, incorporating the 360 primary scalene triangles. The coordinate system for mapping is equally simple, with natural division into steps of  $5^\circ$  RA and  $6^\circ$   $\delta$  (Figure 4). Most significantly, the OED model has no requirement for spherical geometry. In combining simple arithmetical and geometrical approaches, the OED model therefore offers evidence for an early transitional stage prior to adoption of the sphere. This overall perspective is consistent with a comment of Plutarch:

The Pythagoreans (*Puthagoreioi*) embellished (or ‘honoured’ etc, *ekosmēsan*) also numbers and figures (*schēmata*) with the appellations of the gods. The equilateral triangle (*isopleuron trigōnon*) they called Athena, born from the head (*koruphagenē*) and third-born (*tritogeneian*), because it is divided by three perpendiculars (*kathetois*) drawn from its three angles (*On Isis and Osiris* 381f, trans. Babbitt, 1936, pp. 176–177).

Based on Plutarch’s statement: a) the geometry of the triangle was aligned with Pythagorean theology, highlighting its sacred importance, b) those concerned were named by ‘the more elevated form *Puthagoreioi* not the lower form *Puthagorikoi*’ (Nagy, 2013), and c) they already divided the equilateral triangle into the six primary scalene triangles. As Plutarch elsewhere commented, much was deliberately left unsaid (*The Obsolescence of Oracles* 417b, cf. 416d).

### S3.6. Further indications of OED geometry in Mesopotamian and Greek astronomy.

The following examples may be briefly mentioned as providing further connections between ancient astronomy and the geometry of the OED:

- a. **Path of the Moon and ‘Three stars each’ configuration:** MUL.APIN mentions 18 constellations in the ‘Path of the Moon’ (Tablet I, iv.31–iv.39, Hunger and Pingree 1989, pp. 67–69), which could allude to the 18 equilateral triangles of the OED along the Path of Anu. The constellations listed are not evenly spaced along the ecliptic. However, this is typical in such lists, such as the Babylonian ‘3-stars each’ arrangement (e.g. van der Waerden 1974, pp. 64–66). In that case, 36 constellations/stars are listed in 3 rows of 12. Natural division of the OED would similarly explain this orientation of 36 constellations.
- b. **Number of constellations in the Paths of Enlil, Anu and Ea:** There is a close relationship between the number of constellations listed in MUL.APIN in the Paths of Enlil, Anu and Ea, and the Arctic zone (Tablet I, i.1–ii.35, Hunger and Pingree 1989, 18–39) and the number of primary equilateral triangles of the OED. The numbers are as follows: **Arctic zone:** MUL.APIN 6 constellations (included with Path of Enlil), OED 6 equilateral triangles; **Path of Enlil:** MUL.APIN 26 constellations (non-Arctic), OED 15 equilateral triangles; **Path of Anu:** MUL.APIN 19 constellations, OED 18 equilateral triangles; **Path of Ea:** MUL.APIN 15 constellations, OED 15 equilateral triangles; **Antarctic zone:** MUL.APIN 0 constellations; OED 6 equilateral triangles. As constellations could not be seen in the Antarctic zone from  $36^\circ$ N, these last six appear to have been allocated to increase the tally for the Path of Enlil, together with an additional six. This makes a total of 66 constellations listed here in MUL.APIN, as compared with a

total of 60 equilateral triangles on the OED. Expressed as a correlation with  $n=5$  pairs these data give  $R^2=0.75$  and  $P=0.057$ , based on standard parametric statistics.

- c. **‘Three-stars each’ configuration with 30 stars:** Oelsner and Horowitz (1997/1998) describe two Babylonian tablets (HS1897 and BM55502), the first from around 1500–1000 BCE, which imply star lists consisting of 30 constellations oriented as 10 stars in each of the Paths of Anu, Enlil and Ea. The authors show that this format existed simultaneously to the more usual ‘three-stars each’ system of 36 constellations/stars. These 30-star lists support the idea of a 10 month division of the year which can also be achieved using the OED model (see Figure 6), in which case RA necessarily divides into  $6^\circ$  steps and  $\delta$  into  $5^\circ$  steps (cf. below).
- d.  **$6^\circ$  and  $5^\circ$  division of the sphere:** The Greek mathematician Erastheneus was credited by Strabo as the person who first divided the celestial circle into 60 parts, describing the tropics of Cancer and Capricorn as being four ‘parts’ from the equator (i.e.,  $\pm 24^\circ \delta$ , see Dekker 2013, pp. 32–33). Geminus and Macrobius used the same approach, also placing the ever visible Arctic Circle at six parts from the pole (i.e.,  $\pm 54^\circ \delta$ , Geminus 2016, p. 212; Macrobius 1952, pp. 202–209). This system of  $6^\circ$  units using the sexagesimal system seems to be Babylonian in origin (Neugebauer 1975, p. 590; Dekker 2013, p. 33). In particular, it is notable that this system of  $6^\circ$  steps was applied specifically to measure *declination*, while RA was recorded in MUL.APIN using  $5^\circ$  steps. This matches exactly to the natural divisions of the main OED projection used here (Figures 4 and 5). Derivation from the OED of the traditional Greek division of  $\delta$  is also supported by their locating the Arctic Circle at  $\pm 54^\circ$  (with  $36^\circ$  N as the ‘ideal latitude’ for observation) and by their setting of the tropics at  $\pm 24^\circ$ ). The requirement of the OED for such  $5^\circ$  RA and  $6^\circ$   $\delta$  steps (when oriented to divide the year into 12 months) may explain these boundary choices by ancient astronomers. (Note that there is much less evidence for use of the contrasting 10-month orientation of the OED with  $6^\circ$  RA and  $5^\circ$   $\delta$  steps, though see point c. above and main discussion).
- e. **Geometric division of the ecliptic:** Hunger and Pingree (1999, pp. 252–253) give examples of how the Mesopotamians used step-functions to describe cyclic phenomena that proceeded at different speed through their circuits. For example, such a step-function might explain the varying delay in the timing of VMR for the constellations listed at MUL.APIN ii.36–iii.12 or the skewness of the OED model (Supplementary Section 3.3). Two of the functions listed are of special interest in showing resonances with the OED:
- i. For Mars, a function has 6 steps of  $60^\circ$  RA, with this timing matching to the 1’ N-S sectors of the OED. The steps follow the six apices of the OED pentagonal pyramids, equivalent to a line that zig-zags between  $+18^\circ$  and  $-18^\circ \delta$  along the Path of Anu. The line descends to  $-18^\circ \delta$  at Sirius and (following another descent via Antares, Mars’ analogue) ascends to  $+18^\circ \delta$  at Altair, linking to the great cosmic arrows of the OED.
  - ii. For Jupiter, another function has 6 steps of RA, but this time of unequal duration. The rather ‘curious’ timing noted by Hunger and Pingree (1999) was left unexplained, but is consistent with spacing around the OED. It follows a line that crosses the Path of Anu with opposite  $\delta$  to the NGE. The  $\delta$  of this line again descends (through Taurus and Gemini) on approach to Sirius and ascends (out of Scorpio) on approach to Altair.

While the meaning of these step-functions remains unclear, the implication is that the geometric characteristics of the OED may also have informed their setting.

- f. **Orientation of other constellations to features of the OED:** Examination of Figures 4 and 5 and Supplementary Figure SF6 (below) shows several further points of alignment of the constellations with the geometry of the OED. This is particularly visible in the angle of the lower edge of Taurus, the position of the corner stars of Cancer and in the three sections of Eridanus. Further alignments occur in other constellations (e.g., Delta, Orion, Hydra, Crater), which provide an opportunity for further investigation.

### S3.7 Reflection in relation to the evaluation criteria

Considering the nine evaluation criteria, it is elsewhere found that evidence from Philolaus, Theodorus of Soli, Plato, Plutarch, Alcinous, Al-Kindī, Ficino and Pacioli, combines to make a convincing case to affirm Q1 (historical awareness of the OED as a cosmological model) (*Elevated dodecahedron*, forthcoming). By contrast, that study did not find sufficient evidence that the OED was (still) recognized as a basis to map the heavens (Q2). Here I address Q2 based on the astronomical/geometrical evidence of the OED, and then briefly address Q3 (early use of geometrical approaches).

#### S3.7.1 Q1: Was the OED recognized as a basis to map the heavens?

**Criterion 1: Inclusion of a coherent theoretical underpinning in relation to context.** As noted in the introduction, the present findings were not the result of a chance examination, but drew on a clear theoretical foundation that it ought to be possible to construct the dodecahedral All from the Platonic primary triangles. While this is hinted by *Timaeus* 32c, my starting point was an expectation of parallels between Plato's elemental geometry and the elements as treated in ancient Greek and Arabic alchemy (S3.1). The likely numerical attractiveness of the OED to an ancient mind-set interested in number symbolism provided the basis to persist, informed by reflection on the elevated dodecahedra at St. Mark's Venice. Together with the juxtaposition of macrocosm-microcosm in the *Timaeus* and the partial 12-fold symmetry of the OED, it was this theoretical and observational underpinning that gave me confidence to explore the OED further. Criterion 1 is thus fully satisfied.

**Criterion 2: Inclusion of quantitative evidence that is applied to provide statistical assessment.** This has been provided with a focus on the unequal lengths of the zodiac constellations. It should be noted that: a) the statistical comparison of the zodiac constellations with the OED model was possible even without mapping the OED; b) the correlation is already statistically significant (with over 99% confidence that it is not a chance result) without any assumptions (i.e., excluding the equinoctial constellations); c) the statistical comparison is even stronger once a correct assumption is made concerning the OED model 2' boundaries for the equinoctial constellations. Criterion 2 is thus fully satisfied.

**Criterion 3: Inclusion of qualitative evidence in relation to one or more features.**

The OED model provides multiple examples, including: a) the close fit of the model to the Paths of Anu, Ea and Enlil (including the number of constellations in MUL.APIN compared with the 60 equilateral triangles, Supplementary Section S3.5b), b) the way that the model

explains 36° N as an ‘ideal latitude’ in Mesopotamian/Greek astronomy, since this matches the OED setting of 54° N/S for the Arctic and Antarctic circles, and c) natural division of the OED into 6° steps  $\delta$  and into 5° RA steps, as seen in both Babylonian and Greek astronomy. Orientation around the prytany poles could also explain early Babylonian 10 x 3 stars each star maps (Oelsner and Horowitz, 1997/1998, see Supplementary Section S3.5). Criterion 3 is evidently satisfied based on many qualitative points of correspondence.

**Criterion 4: Inclusion of multiple layers of evidence that together establish a coherent picture.** This criterion can be considered as a stronger version Criterion 3, where it is possible to link multiple layers of evidence. The simple illustration of testing a loaded coin (see Supplementary Methods S1.3), represents a rather crude approach, but may be helpful when considering qualitative evidence where formal statistical testing is not feasible. An example is provided by the ‘cosmic arrows’ formed by combining the adjacent zodiac constellation pairs due to the partial symmetry of the decorated OED. Six linked features may be noted in the overall group of correspondences (Table ST7).

If each of these features were assigned a 50% probability of occurring by chance, with  $n-1$  degrees of freedom (i.e.,  $0.5^{(n-1)}$ ), then the probability of all these occurrences occurring by chance would  $P=0.03$  (i.e., 97% confident that this is not a chance result). Although the approach is extremely simplistic, it illustrates how one or two qualitative correspondences could easily be the result of chance coincidence. By contrast, a correspondence of six related features can be considered as very unlikely to have occurred by chance. The picture painted is equally coherent: that the Greek myth recorded by Porphyry and Macrobius (even though of late date) has plausible antecedents in both Greek and Mesopotamian astronomy and in the OED geometric framework. Whether or not one accepts the implications, at least Criterion 4 is satisfied.

**Criterion 5: Linking of a sequence of several steps of evidence, showing predictive capability.** Predictive capability of a model may be considered as one of the strongest features to support its acceptance. The simplest examples concern qualitative findings, where first findings provide the basis for sensible hypotheses to be followed-up. This can be illustrated by my own expectation that Greek alchemical treatment of the elements (i.e., preparation of aether as the alchemical quintessence by marrying the elements) would have a parallel in the geometrical quintessence (dodecahedron, aether), produced by marrying or recombining the geometric elements (cf. *Timaeus* 56e). This expectation was fully met by the OED made from 360 primary scalene triangles. This finding led to the expectation that the numerical resonances of the OED (5, 12, 30, 60, 360 etc) would have been appealing to an ancient mind-set interested in number symbolism, such as attributed to the Pythagoreans. It was only much later that this expectation was found to be met by the likes of Plutarch, Alcinoüs, al-Kindī and Ficino in their descriptions of the OED (*Elevated dodecahedron*, forthcoming). This sequence of finding and further hypothesis has been apparent throughout the study, including: a) the expectation that the OED could be used as a mapping framework and b), given that the zodiac constellations fit within the OED framework, then it can be expected that other constellations will also do so. Overall, it is evident that Criterion 5 is satisfied.

**Table ST7:** Correspondences noted between the Greek myth, constellations and the OED model sectors.

	Cancer / Summer	Capricorn / Winter
Greek myth (Path of Souls)	Soul's descent (Path down Milky Way)	Soul's ascent (Path up Milky Way)
Main star and Mesopotamian constellations	<ul style="list-style-type: none"> <li>• 'The Arrow' (<sup>[mul]</sup>KAK.SI.ŠA], Sirius)</li> <li>• Illustrated as a downward pointing arrow</li> <li>• Associated with the bow/arrow Ninurta</li> </ul>	<ul style="list-style-type: none"> <li>• 'The Eagle' (<sup>[mul]</sup>TI<sub>8</sub><sup>[mušen]</sup>, Altair)</li> <li>• Associated in Babylonian astronomy with Marduk (Jupiter). Illustrated by an upward pointed arrow ('Spade')</li> <li>• Adjacent to Sagitta ('the Arrow') in Greek astronomy</li> </ul>
OED sectors	Downward-pointing cosmic arrow (see Figure 5; cf. SF6)	Upward-pointing cosmic arrow (opposite to Figure 5; cf. SF6)
Possible common theme?	Integration of sky and earth (cf. Ninurta crowned with the heavens and shod with the netherworld; Rochberg, 2020, pp. 308–309)	Separation of sky and earth (cf. Marduk splits Tiamat to form heaven and earth; Rochberg, 2020, p. 308)

The application of Criterion 5 also points to future opportunities. For example, the use of many faint stars would have given more flexibility in designing constellations. This offers a further hypothesis for future testing: that faint constellations would more easily align with the OED framework than constellations dominated by a few bright stars.

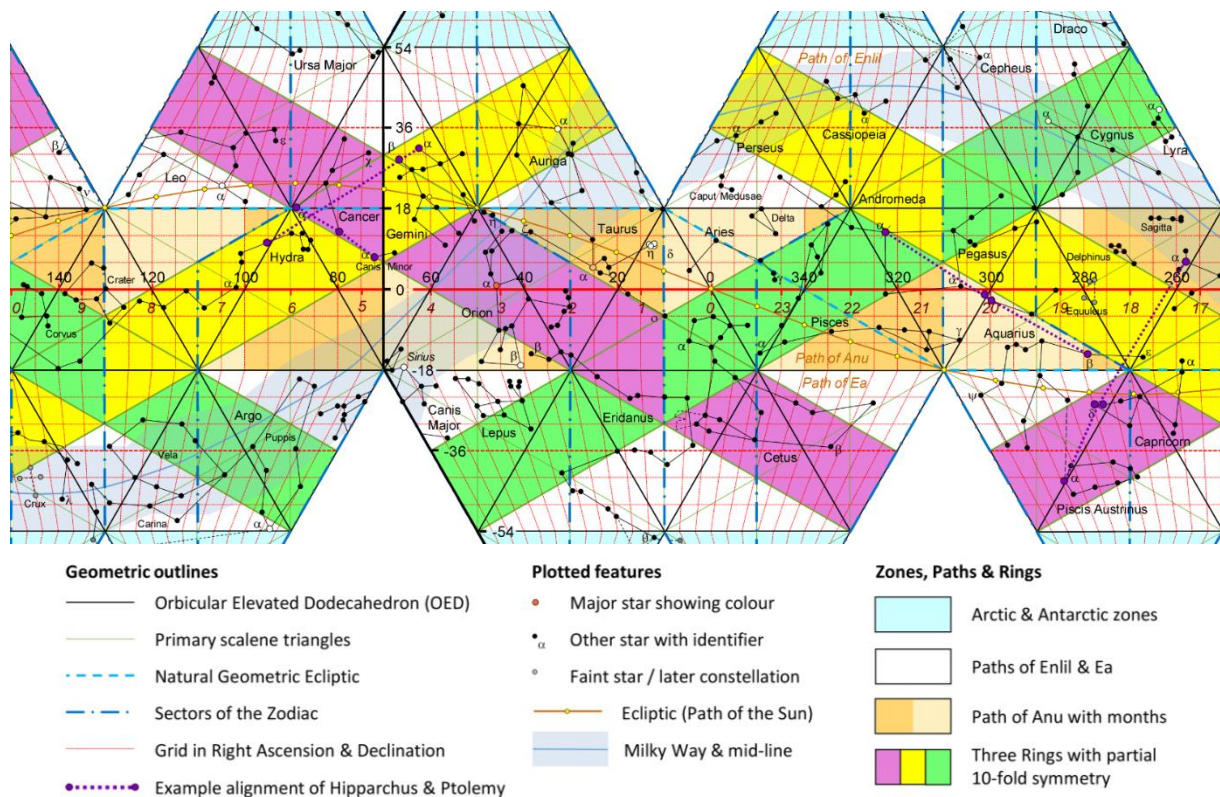
**Criterion 6: Inclusion of a quantitative/qualitative model as a basis for robust predictive capability.** Where the evidence allows, this must be considered as the most powerful of the criteria, especially where quantitative data can be compared with an independent model. The good news is that both model and independent data are available through the OED and the classical constellations, respectively. The most obvious example, concerns my early mapping of the OED, which showed that the partial 12-fold rotational symmetry, in crossing the diagonal of the natural geometric ecliptic, leads to expectation from the model that: a) some zodiac constellations may be longer than others, and b) if the model is oriented correctly, it should be possible to predict the long and short zodiac constellations. The statistical comparison of Supplementary Figure SF4 more than satisfies the first of these, while application of the same data in the polar plot (Figure 3) shows how the 'fingerprint' of the model is closely matched by the constellation data.

An example of qualitative predictive capability can be found when considering the alignments of the constellations in relation to the OED framework, especially around the 'three rings' that follow the prytany equators. Several such alignments are seen in Figure 5, with others illustrated in Supplementary Figure SF6, which shows the OED cosmos unwrapped as a net, including the main 5° and 6° divisions of RA and  $\delta$ , respectively. Such alignments were presumably useful to orient observations across the sky.

I subsequently noted that Ptolemy had recorded a selection of star alignments as part of his description of observations from Hipparchus in relation to the question of precession (*Almagast* 7.1). Since Ptolemy and Hipparchus were interested in ancient lines of stars, it seemed a reasonable hypothesis that some of their star lines might retain information from the

(older) OED model, even though they were using later spherical geometry. This expectation turned out to be the case, as illustrated by Supplementary Figure SF6. Four examples of the star alignments listed by Hipparchus (H) /Ptolemy (P) are shown: i,  $\alpha$  Gemini to  $\theta$  Hydra (P4); ii,  $\alpha$  Canis Minor to  $\alpha$  Cancer (H1); iii,  $\alpha$  Aquila to  $\alpha$  Piscis Austrinus (P21); and iv,  $\beta$  Aquarius to  $\alpha$  Andromeda (H11). Other alignments include: v,  $\mu$  Serpens to  $\alpha$  and  $\beta$  Libra (H6); vi,  $\alpha$  and  $\beta$  Libra to  $\pi$  Hydra (P13); vii,  $\alpha$  Virgo to  $\beta$  Bootes (P10); viii,  $\beta$  Aquarius to  $\epsilon$  Pegasus (H10). Such alignments tend to suggest that the star-alignment records of Ptolemy and Hipparchus do indeed recall some vestiges of the earlier OED system, consistent with current ideas that both these writers were influenced (directly or indirectly) by antecedent Babylonian sources (e.g., Hoffmann, 2018). The examples show how Criterion 6 is met.

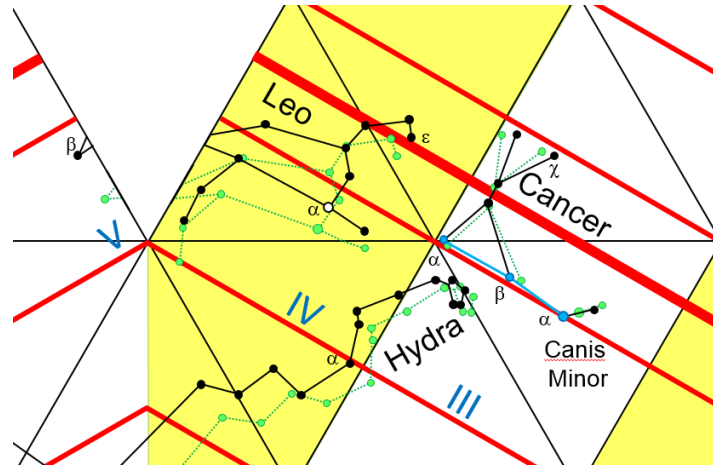
A potential criticism of this observation is that only 8 out of the 41 alignments of Hipparchus and Ptolemy match closely to the OED framework (~20%). Further work is needed to confirm that this is not a chance result (cf. Supplementary Figure SF8A). This should consider not just the angles of these star-lines, but different dates and their position in relation to the key paths (e.g., Hipparchus alignments H1, H6 and H11 all occur at the lower NW-SE edge of the three northerly junctions of the Three Rings with 10-fold symmetry).



**Supplementary Figure SF6:** Partial view the OED projection showing star positions as viewed from Earth for 1200 BCE, where 0° Right Ascension is here set at the mid-point of the OED 20° sector of Aries. Four example star alignments noted by Hipparchus and Ptolemy are shown (*Almagast 7*). (Image © Mark Sutton, 2021).

**Criterion 7: Ability to demonstrate expected degradation of the model.** This is probably my favourite criterion, as its acceptance demonstrates, not only that we can predict certain observations based on a model, but we have some understanding of when and why the model will perform better or worse. The most obvious example with the OED model concerns the

fitting of the constellations considering RA in relation to date, given precession of the equinoxes. As discussed, the model appears to fit best for around 1200–1100 BCE. This suggests that the model performance may also be deliberately degraded by choosing an incorrect date. An illustration of the effect is shown in Supplementary Figure SF7, which considers the case of the constellations Leo and Cancer for an unfeasibly late date of 140 CE (i.e., contemporary with Ptolemy). While the alignments for Cancer are only slightly degraded, the alignment of Leo along the OED framework is completely lost. This expected degradation of the model performance shows how Criterion 7 is met.

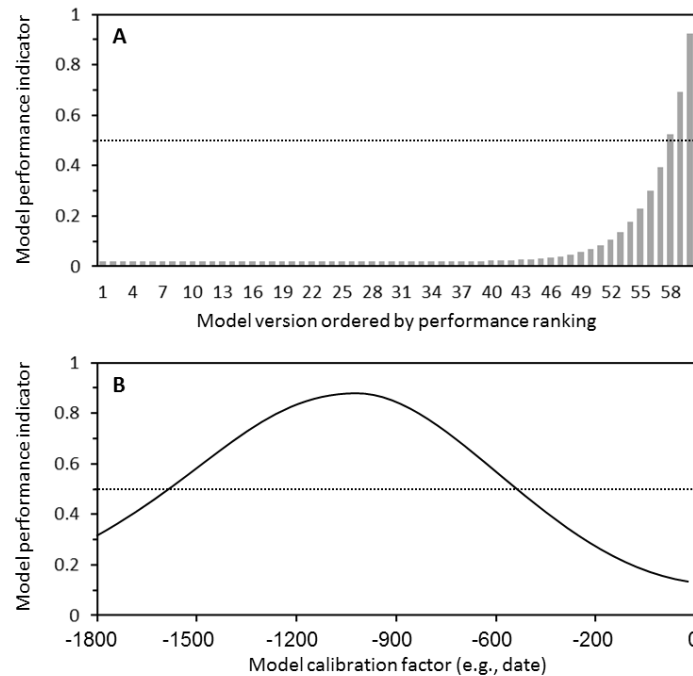


**Supplementary Figure SF7:** Section of the dodecahedral projection showing prytany sectors III-V, where each 36 day period is shaded alternately white-yellow (cf. Figure 6). The bold red line shows the prytany equator where the ‘prytany poles’ are at Cepheus and Carina. The stars in black and blue are plotted for 1200 BCE (setting  $0^\circ$  RA at the mid-point of the 20-day sector of Aries). The blue shaded stars indicate the first alignment noted by Hipparchus (Almagast 7). The green constellation outlines are plotted for the time of Ptolemy (140 CE, where  $0^\circ$  RA is set at the start of the 30-day sign of Aries, i.e., 20 days earlier than for 1200 BCE). (Image © Mark Sutton, 2021)

It is important to distinguish such predictable differences in model performance from the occasional case of acceptable performance as a result of trying a large number of arbitrary options. This point is illustrated visually in Supplementary Figure SF8. In both parts of the figure, the performance of an imaginary model is given using a model performance indicator, rated 0–1, where any value greater than 0.5 is considered to be acceptable. In part A, there are 60 arbitrary options, of which three are found to be acceptable. In part B, a single model calibration factor is used, such as supposed model date, with this example showing acceptable results for around -1600 to -500.

The reality for Figure SF8A is that there is no true relationship. With three out of 60 results ‘acceptable’, the model shows an acceptable result purely by chance for 5% of the arbitrary options (i.e., ‘false positives’ also known as Type 1 errors). The example may explain how Kepler managed to find good agreement with the planetary spacing by considering multiple arbitrary arrangements of the Platonic solids. Although Kepler offered arguments as to why each Platonic solid should be linked to each interval (see Kepler, 1997, pp. 12, 114–116), the arguments are questionable and the suspicion is that he explored multiple options, not just of the order of the polyhedra ( $5!$ , i.e. 120), but also variants, such as including spacing of the Moon along with the Earth and different ways of averaging (Field, 1982, pp. 559, 567).

By contrast, Figure SF8B illustrates a valid case of model tuning, where the performance of the model is dependent on a model calibration factor, such as date. This is comparable to considering the overall fit of the classical constellations to the OED model. As such changes are well understood (e.g., with time-dependent constellation data available using software such as Stellarium), this provides a valid basis for tuning, where the imaginary model performs best for a date of around -1000.



**Supplementary Figure SF8:** Illustration of the variation in performance for two imaginary models: **A.** Consideration of 60 arbitrary options in this example leads by chance to three model versions passing a threshold of 0.5 for acceptable model performance, even though there is no true relationship. **B.** Consideration of valid tuning of model performance according to one numerical calibration factor, such as model date as shown here. The model meets the performance threshold for a wide range of dates, while degrading in an expected fashion.

**Criterion 8: Demonstration of an internally consistent whole.** Considering all the evidence together, it is possible to produce a coherent picture. It appears that at some point in time (presumably well before 1200 BCE) Mesopotamian, Egyptian or other astronomers started using the OED as a simple geometric framework for their astronomy and cosmology (e.g., paths of Anu, Ea, Enlil; arrow symbolism). As the OED model is simple, spherical geometry or proofs would not have been needed, with arithmetical approaches in geometrical context sufficient. Consistent with a pattern of scribal secrecy (Lenzi, 2013), it appears that the OED model itself was never published by its originators, who used it to design the classical constellations. If the model was indeed originally of Babylonian or Egyptian origin, then its transference to Greece (matching transfer of other cosmological ideas, Horkey, 2009; cf. *Phaedrus* 274c,d; *Epinomis* 986e-987a; Aristotle, *De Caelo* 292a; Strabo XVI.2.24; Diogenes Laertius 1.11) apparently happened as a matter of reserved knowledge. Since the classical constellations as we see them represent a known mix of Mesopotamian and Greek elements, it seems likely that both traditions knowingly made use of the OED.

Scholars have debated the fact that the *Phenomena* of Eudoxus (c. 350 BCE) appears to date from much earlier than would seem reasonable, to about 1200-1100 BCE (e.g., Schaefer

2004; Duke 2008; cf. Rogers, 1998, pp. 79–81, and references therein, who proposed 2000–1800 BCE). While Schaefer applied a statistical approach to obtain his dating, Duke rejected this conclusion based on his own further statistical analysis and logical arguments, including potential rejection of the data of Eudoxus as unreliable. As Duke (2008, p. 15) commented: ‘setting aside the on-circle data of Eudoxus, no evidence has come down to us suggesting that any culture prior to Eudoxus’ time understood the cosmology of the celestial sphere.’ The present contribution informs this debate with two extra layers: i) OED approximation to the sphere with no requirement for spherical geometry; ii) importance of scribal secrecy (cf. Lenzi, 2013) as part of the ‘paradigm of increasing openness’. In this way ‘first publication’ can be expected many centuries after discovery and original use. Whether or not the picture is accepted, it does at least satisfy Criterion 8.

**Additional Criterion 9: Checking that the finding is not overly dependent on altering or criticizing the original sources.** In examining historical texts relevant to the OED, a related study found that many commentators had concluded that the original authors must have been mistaken about the dodecahedron, instead of embracing the dodecahedron as a puzzle to be solved (*Elevated dodecahedron*, forthcoming). This highlights the need to check that any interpretation is not overly dependent on assuming that the ancients were wrong or that an apparently nonsensical text is corrupt. For example, Duke (2008, p. 17) suggested an option that ‘Eudoxus, or some near contemporary, made errors sufficiently large to account for the observations he used’ (cf. Rogers, 1998, p. 81). The evidence presented here indicates that the puzzle had another solution. By avoiding to assume in the present study that the ancients were in error, Criterion 9 is also satisfied.

Overall, it can be a difficult matter to work out whether or not a case is robust. Nevertheless, the present study meets all nine of the criteria for this question, pointing to the robustness of the discovery that the OED was used by the ancients for mapping the cosmos. Ultimately, I expect that wider acceptance will depend on further application of Criteria 5 and 6: where the model is found to predict and explain other things beyond those identified here.

### **S3.7.2. Does awareness of the OED model by the ancients indicate early use of geometrical approaches?**

The evaluation criteria can be applied more briefly for this question than the previous. This is because the question is answered by inference rather than being entirely dependent on fresh evidence. In effect, Criterion 1 is met by the prior demonstration that the OED was used as a mapping framework. Since the OED is a geometric construct, this implies by definition that the ancients made some use of geometrical approaches. Criteria 2 and 4–7 are thus incorporated into the background that addresses Criterion 1.

It could be criticised that the claim to geometrical approaches for 1200 BCE flies in the face of evidence that Babylonian astronomy was limited to arithmetical approaches. Part of the resolution to this problem seems to be that the OED itself is an extremely simple geometric construction, for which neither spherical geometry nor geometrical proofs are needed

(Supplementary Section 3.5). The interpretation contributes to an internally consistent whole (meeting Criterion 8), while raising no concerns about Criterion 9.

Comparison of the present findings with modern scholarly opinion also suggests a tenth criterion for use in future studies.

**Additional Criterion 10: That the finding is not overly dependent on arguments from silence.** In particular, any interpretation that gives more weight to missing evidence than conflicting available evidence should be considered unreliable, especially in the context of the paradigm of increasing openness. For example, having recognized that the evidence of Eudoxus suggests a date of ~1100 BCE, Duke (2008, pp. 15–16) sets out to show statistically that this early dating is not significantly different to the time of Eudoxus (~350 BCE), then noting that: ‘it strains credulity to the breaking point that each and every source we know from the time before Eudoxus might have known about the celestial sphere in all its details, but either chose not to write anything about it, or if they did, it has not reached us, even indirectly through intermediate sources such as Hipparchus.’ While we may sympathise with Duke’s difficulty, his position represents a case of prioritizing *argumentum ex silentio* above the substantive evidence. With the benefit of hindsight, I would suggest that the design of the classical constellations described by Eudoxus was informed by the OED model as a matter of reserved knowledge, fully consistent with the early dating. A comparable example is provided by Zhmud (2012, pp. 239–251), who presents a wealth of evidence from ancient Greek authors that the Egyptians were the source of Greek geometry. Yet Zhmud emphasizes: ‘What of this can we relate to Egyptian geometry? Absolutely nothing... neither did the Egyptians ever engage in comparing the size of angles... In Egyptian mathematics, however there is nothing indicating familiarity with ... the theorem of Pythagoras’ (pp. 246–247). In so doing, he prioritizes the argument from silence above the extant reports. The net result also informs Criterion 9, with both Zhmud and Duke being over-ready to assume that the ancient authorities were mistaken.

Finally, I conclude that there is no contradiction with the oft-quoted scholion to Euclid’s *Elements* 13.1 (ed. Heiberg, 1888, Vol. 5, p. 654): ‘In this book, that is to say the 13<sup>th</sup>, are written-down/described the so-called Platonic figures, which are not his, three of the mentioned figures are from the Pythagoreans, the cube and the pyramid and the dodecahedron, of Theaetetus are the octahedron and the icosahedron’ (*En toutō tō bibliō, toutesti tō ig, graphetai ta legomena Platōnos e schemata, ha autou men ouk estin, tria de tōn proeirēmenōn e schēmatōn tōn Puthagoreiōn estin, ho te kubos kai he puramis kai to dōdekaedron, Theaitētou de to te oktaedron kai to eikosaedron*). Whatever the exact intended meaning (from basic discovery to geometric proof, see Introduction), the author is clear that the dodecahedron was already known to the Pythagoreans (as also recorded of Hippasus by Iamblichus; see Section 5.4). In the absence of explicit accounts, we depend on the evidence from astronomy for its earlier history.

## Bibliography to the Supplementary Information

- Damascius, *The Greek Commentaries on Plato's Phaedo. Vol. 1. Olympiodorus; Vol. 2. Damascius.* (2<sup>nd</sup> edn). ed. and trans. L.G.W. Westerink (Westbury: Prometheus Trust, 2009).
- Florence Daily News, *The Medici Chapels and Michelangelo's 'crown'* [online] (17 January 2013). Accessed June 2014. <http://www.florencedailynews.com>
- Geminus, *Introduction to the Phenomena*, trans. and study J. Evans and J.L. Berggren (Princeton, NJ: Princeton University Press, 2006).
- Hershbell, J.P. 'Democritus and the beginnings of Greek alchemy', *Ambix*, Vol. 34, (1987), pp. 63–78.
- Hoffmann, S.M., 'The genesis of Hipparchus' celestial globe', *Mediterranean Archaeology and Archaeometry*, Vol. 18, (2018), pp. 281–287. doi.org/10.5281/zenodo.1477980
- Høyrup, J., What is "geometric algebra", and what has it been in historiography? (Paper presented at Histoire de l'historiographie de l'algèbre, Paris, France), at [https://rucforsk.ruc.dk/ws/portalfiles/portal/59332142/Hoyrup\\_What\\_is\\_Geometric\\_Algebra\\_Prprt.PDF](https://rucforsk.ruc.dk/ws/portalfiles/portal/59332142/Hoyrup_What_is_Geometric_Algebra_Prprt.PDF) [accessed on 6 Jan. 2021].
- Hunger, H. and Pingree, D., *Astral sciences in Mesopotamia* (Leiden: Brill, 1999).
- Jones, A., On Babylonian astronomy and its Greek metamorphoses, in F.J. Ragep, S.P. Ragep, S.J. Livesey, (eds.), *Tradition, Transmission, Transformation: Proceedings of Two Conferences on Pre-Modern Science Held at the University of Oklahoma.* (Leiden: Brill, 1996), pp. 139–155.
- Kepler, J., *The harmony of the world*, trans. E.J. Aiton, A.M. Duncan and J.V. Field (Philadelphia: American Philosophical Society, 1997).
- Lovi, G., 'The Classical Sky', *Sky & Telescope* (July 1988), pp. 55–56.
- Martelli, M. 'The four books of pseudo-Democritus', *Ambix*, Vol. 60, (Supplement 1) (Leeds: Maney Publishing, 2013), 298 pp.
- Nagy, G., Comments on Plutarch's Essay *On Isis and Osiris* [6<sup>th</sup> edition, 2013] [http://nrs.harvard.edu/urn-3:hnc.essay:Nagy.Comments\\_on\\_Isis\\_and\\_Osiris.1999-](http://nrs.harvard.edu/urn-3:hnc.essay:Nagy.Comments_on_Isis_and_Osiris.1999-) (Accessed 20 January 2021).
- Neugebauer, O., *A history of ancient mathematical astronomy.* 3 vols. (Berlin and New York: Springer-Verlag, 1975).
- Rochberg, F., Mesopotamian cosmology, in D.C. Snell, (ed.), *A Companion to the Ancient Near East, Second Edition* (Hoboken, NJ: John Wiley & Sons, Inc., 2020), pp. 305–320. doi.org/10.1002/9781119362500.ch18
- Rogers, J.R., 'Origins of the ancient constellations: II. The Mediterranean traditions', *Journal of the British Astronomical Association*, Vol. 108, (1998), pp. 79–89.
- Stapleton, H.E. and Azo, R.F. 'An alchemical compilation of the thirteenth century, A.D.', *Memoirs of the Asiatic Society of Bengal*, Vol. 3, (1910), pp. 57–94.
- Sutton, M.A., van Dijk, N., Levy, P.E., Jones, M.R., Leith I.D., Sheppard, L.J., Leeson, S., Tang, Y.S., Stephens, A., Braban, C.F., Dragosits, U., Howard, C.M., Vieno, M., Fowler, D., Corbett, P., Naikoo, M.I., Munzi, S., Ellis, C.J., Chatterjee, S., Steadman, C.E., Möring, A. and Wolseley, P.A. 'Alkaline Air: changing perspectives on nitrogen and air pollution in an ammonia-rich world', *Philosophical Transactions of the Royal Society of London A*, Vol. 378, (2020), Article 20190315. doi.org/10.1098/rsta.2019.0315
- Sutton, M.A., Erisman, J.W., Dentener, F. and Moeller, D. 'Ammonia in the environment: from ancient times to the present', *Environmental Pollution*, Vol. 156, (2008), pp. 583–604. doi.org/10.1016/j.envpol.2008.03.013
- Sutton, M.A., Howard, C., Erisman, J.W., Billen, G., Bleeker, A., Grennfelt, P., van Grinsven, H. and Grizzetti, B. (eds.) *The European Nitrogen Assessment.* (Cambridge: Cambridge University Press, 2011).
- van der Waerden, B.L., *Science Awakening. Vol. 2., The birth of astronomy.* (Leyden: Noordhoff International; New York: Oxford University Press, 1974).
- Viano, C., 'Les alchimistes Gréco-Alexandrins et le Timée de Platon', in C. Viano, (eds.), *L'alchimie et ses racines philosophiques: La tradition grecque et la tradition arabe* (Paris: Librairie Philosophique J. Vrin, 2005), pp. 91–107.
- Viano, C., Greco-egyptian alchemy, in A. Jones and L. Taub, (eds.), *The Cambridge History of Science, vol.1: Ancient Science* (Cambridge: Cambridge University Press, 2018), pp. 468–492.